

Expression of PD-1/PD-L1 and Inflammasome Mediators in Oral Squamous Cell Carcinoma: Correlation with Key Clinical and Pathological Variables

Oscar Fraile-Martinez*

 <https://orcid.org/0000-0002-4494-6397>
Instituto Ramón y Cajal de Investigación Sanitaria
 <https://ror.org/03fftr154>
University of Alcalá
 <https://ror.org/04pnm0e78>

Cielo Garcia-Montero*

 <https://orcid.org/0000-0001-6016-7855>
University of Alcalá
 <https://ror.org/04pnm0e78>
Instituto Ramón y Cajal de Investigación Sanitaria
 <https://ror.org/03fftr154>

María Jesus Garrido-Gil

 —
University of Alcalá
 <https://ror.org/04pnm0e78>
Instituto Ramón y Cajal de Investigación Sanitaria
 <https://ror.org/03fftr154>

Laura Ríos-Espinosa

 —
University of Alcalá
 <https://ror.org/04pnm0e78>
Instituto Ramón y Cajal de Investigación Sanitaria
 <https://ror.org/03fftr154>

Diego Liviu Boaru

 <https://orcid.org/0009-0003-5909-788X>
University of Alcalá
 <https://ror.org/04pnm0e78>
Instituto Ramón y Cajal de Investigación Sanitaria
 <https://ror.org/03fftr154>



Diego De Leon-Oliva

 <https://orcid.org/0009-0006-2038-1754>
University of Alcalá
 <https://ror.org/04pnm0e78>
Instituto Ramón y Cajal de Investigación Sanitaria
 <https://ror.org/03fftr154>

Patricia De Castro-Martinez

 <https://orcid.org/0009-0002-8591-6116>
University of Alcalá
 <https://ror.org/04pnm0e78>
Instituto Ramón y Cajal de Investigación Sanitaria
 <https://ror.org/03fftr154>

Claude Pereda-Cerquella

 —
University of Alcalá
 <https://ror.org/04pnm0e78>



Majd N. Michael Alhaddadin

 —
University of Alcalá
 <https://ror.org/04pnm0e78>

Silvestra Barrena-Blázquez

 <https://orcid.org/0000-0003-2715-1979>
Instituto Ramón y Cajal de Investigación Sanitaria
 <https://ror.org/03fftr154>
University of Alcalá
 <https://ror.org/04pnm0e78>

Antonio Ríos-Parra

 <https://orcid.org/0000-0002-5863-7851>
University of Alcalá
 <https://ror.org/04pnm0e78>

Laura Lopez-Gonzalez

 <https://orcid.org/0009-0005-1023-7639>
Instituto Ramón y Cajal de Investigación Sanitaria
 <https://ror.org/03fftr154>
University of Alcalá
 <https://ror.org/04pnm0e78>



Luis G . Guijarro

 <https://orcid.org/0000-0003-4979-2136>
Instituto Ramón y Cajal de Investigación Sanitaria
 <https://ror.org/03fftr154>
University of Alcalá
 <https://ror.org/04pnm0e78>



Alejandro Coca

 —
University of Alcalá
 <https://ror.org/04pnm0e78>
Instituto Ramón y Cajal de Investigación Sanitaria
 <https://ror.org/03fftr154>

Víctor Roberto Baena Romero

 <https://orcid.org/0009-0002-7826-421X>
University of Alcalá
 <https://ror.org/04pnm0e78>

Carlos Daniel Padilla Ansala

 <https://orcid.org/0000-0002-9385-9193>
University of Alcalá
 <https://ror.org/04pnm0e78>




María del Mar Royuela García

 <https://orcid.org/0000-0003-1999-9849>
Instituto Ramón y Cajal de Investigación Sanitaria
 <https://ror.org/03fftr154>
University of Alcalá
 <https://ror.org/04pnm0e78>



María Del Val Toledo Lobo

 <https://orcid.org/0000-0001-7222-8096>
University of Alcalá
 <https://ror.org/04pnm0e78>
Instituto Ramón y Cajal de Investigación Sanitaria
 <https://ror.org/03fftr154>

Leonel Pekarek

 <https://orcid.org/0000-0002-5966-9003>
University of Alcalá
 <https://ror.org/04pnm0e78>
Instituto Ramón y Cajal de Investigación Sanitaria
 <https://ror.org/03fftr154>
Hospital Universitario de Guadalajara





Montserrat Chao Crecente

 <https://orcid.org/0000-0002-2517-6809>
University of Alcalá
 <https://ror.org/04pnm0e78>





Ángel Asúnsolo

 <https://orcid.org/0000-0001-7898-4685>
Instituto Ramón y Cajal de Investigación Sanitaria
 <https://ror.org/03fftr154>
University of Alcalá
 <https://ror.org/04pnm0e78>





Melchor Alvarez-Mon

 <https://orcid.org/0000-0001-6599-6169>
University of Alcalá
 <https://ror.org/04pnm0e78>
Instituto Ramón y Cajal de Investigación Sanitaria
 <https://ror.org/03fftr154>
Hospital Universitario Príncipe de Asturias
 <https://ror.org/01az6dv73>

Julio Acero

 <https://orcid.org/0000-0002-0811-1368>
Instituto Ramón y Cajal de Investigación Sanitaria
 <https://ror.org/03fftr154>
University of Alcalá
 <https://ror.org/04pnm0e78>
Hospital Universitario Ramón y Cajal
 <https://ror.org/050eq1942>




Raúl Díaz-Pedrero

 <https://orcid.org/0000-0003-0412-939X>
Instituto Ramón y Cajal de Investigación Sanitaria
 <https://ror.org/03fftr154>
University of Alcalá
 <https://ror.org/04pnm0e78>
Hospital Universitario del Henares
 <https://ror.org/047ev4v84>

Miguel A. Saez

 <https://orcid.org/0000-0002-8389-258X>
University of Alcalá
 <https://ror.org/04pnm0e78>
Instituto Ramón y Cajal de Investigación Sanitaria
 <https://ror.org/03fftr154>

Miguel A. Ortega

 <https://orcid.org/0000-0003-2588-1708>
University of Alcalá
 <https://ror.org/04pnm0e78>
Instituto Ramón y Cajal de Investigación Sanitaria
 <https://ror.org/03fftr154>
Corresponding author: miguelangel.ortega@uah.es

* Equal contribution

 <https://doi.org/10.20883/medical.e1446>

Keywords: oral squamous cell carcinoma (OSCC); histopathology; PD-1/PD-L1; NLRP3 inflammasome; NAIP/NLRC4 inflammasome; clinical variables

Received 2025-10-02

Accepted 2026-02-15

Published 2026-03-31

How to Cite: Fraile-Martinez O, Garcia-Montero C, Garrido-Gil MJ, Ríos-Espinosa L, Boaru DL, De Leon-Oliva D, et al. Expression of PD-1/PD-L1 and inflammasome mediators in oral squamous cell carcinoma: correlation with key clinical and pathological variables. *Journal of Medical Science*. 2026 March;95(1);e1446. <https://doi.org/10.20883/medical.e1446>



© 2026 by the Author(s). This is an open access article distributed under the terms and conditions of the Creative Commons Attribution (CC BY-NC) license. Published by Poznan University of Medical Sciences

ABSTRACT

Objective. Oral squamous cell carcinoma (OSCC) is a leading cause of head and neck cancer morbidity and mortality. This study aimed to explore the relationship between immune checkpoint regulation and inflammasome-related pathways in OSCC, focusing on the Programmed cell death protein 1 (PD-1)/Programmed

cell death ligand 1 (PD-L1) axis and components of the NLR family pyrin domain containing 3 (NLRP3 and NLR family apoptosis inhibitory protein (NAIP) inflammasomes in relation to relevant clinical variables.

Design. This retrospective observational study included 30 patients with OSCC who underwent surgical resection. Histopathological expression of PD-1, PD-L1, NLRP3, Apoptosis-associated speck-like protein containing a CARD (ASC/PYCARD), caspase-1, Interleukin-1 beta (IL-1 β), IL-18, caspase-5, caspase-8, and NAIP was assessed by immunohistochemistry using ordinal scoring. Associations with clinical features were evaluated using non-parametric tests and Spearman correlation analyses. Inter-marker relationships were explored using correlograms and heatmaps, with stratification by tumour grade. Exploratory binary logistic regression models were applied to examine associations between marker expression and selected clinical variables.

Results. Marker expression showed significant associations with tumour grade, relapse, vascular invasion, and oral hygiene, whereas age, sex, smoking status, alcohol consumption, and other clinicopathological variables were not significantly related. Higher-grade tumours exhibited stronger and more extensive inter-marker correlations, suggesting coordinated activation of immune and inflammatory pathways. Increased expression of PD-L1, NAIP, NLRP3, caspase-1, caspase-5, and PYCARD was associated with higher tumour grade, while relapse was linked to elevated expression of NAIP, NLRP3, caspase-1, and IL-18. Poor oral hygiene was inversely associated with the expression of multiple immune and inflammasome-related markers, whereas vascular invasion correlated with broadly increased marker expression.

Conclusions. These findings indicate that immune checkpoint signalling and inflammasome-related pathways are closely associated with aggressive clinicopathological features in OSCC. The coordinated expression patterns observed support a role for inflammation-driven immune modulation in disease progression. Although exploratory, this study provides a framework for future investigations aimed at validating these pathways as biomarkers or therapeutic targets in larger cohorts.

Introduction

Oral squamous cell carcinoma (OSCC) accounts for more than half of head and neck squamous cell carcinomas (HNSCC), which develop in the squamous epithelium of the lip or oral cavity [1]. OSCC represents over 90% of all oral cancers [2] and according to recent global cancer statistics approximately 389,485 new cases of lip and oral cavity cancer were diagnosed worldwide, with an estimated 188,230 deaths, ranking as the 16th tumor in terms of incidence and the 15th in terms of mortality [3]. The highest incidence rates are observed in South Central and Southeast Asia, Eastern Europe, and Australia/New Zealand, with a greater representation in low/medium Human Development Index (HDI) countries and in men over 50 years of age [3,4]. Five-year survival rates for OSCC is highly variable according to the diagnosis, ranging from 90% in earlier stages to about 30% in advanced stages [5]. Major risk factors include tobacco use, alcohol consumption, betel quid chewing, poor oral hygiene, human papillomavirus (HPV) infection (though less than in oropharyngeal cancers), immunosuppression and a diet poor in vegetables and fruits [6,7].

Notably, the disease burden is expected to rise due to aging populations and persistent exposure to risk factors in high-incidence regions [6].

Histologically, OSCC is classified primarily as keratinizing or non-keratinizing squamous cell carcinoma, with further gradations based on differentiation (well-, moderately-, or poorly-differentiated) [8,9]. The most common anatomical location of OSCC is the posterior lateral border of the tongue accounting for approximately half of all OSCC occurrences. Following this, the mouth floor, the soft palate, the gingiva, the buccal mucosa, and the hard palate [10]. Anatomopathologically, these tumors show invasive growth, keratin pearl formation, an increase in nuclear cytoplasmic ratio, intercellular bridges, nuclear chromatin irregularities and increased mitotic figures as the most common findings [11]. Clinically, OSCC is often diagnosed at advanced stages, with local invasion and regional lymph node metastases being common. Biological characteristics such as perineural invasion, lymphovascular spread, and the presence of high-risk molecular markers contribute to prognosis and therapeutic decisions [12,13] Despite surgical and adjuvant therapy advances, recurrence rates and

mortality remain substantial, emphasizing the need for better molecular understanding.

The tumor microenvironment in OSCC is increasingly recognized as a critical determinant of disease progression, therapeutic response, and patient outcomes. Chronic inflammation and immune evasion are considered two hallmarks of cancer [14], playing a pivotal role in OSCC carcinogenesis [15,16]. The analysis of inflammatory biomarkers—such as those involved in inflammasome activation and immune checkpoint regulation—can yield insights into the mechanisms of tumor progression and therapy resistance [17]. Studying these biomarkers in tumor tissues allows for the correlation of molecular patterns with clinical and pathological variables (e.g., tumor stage, grade, lymph node status), helping identify predictive and prognostic indicators [18, 19]. Additionally, exploring these markers could contribute to the development of personalized immunomodulatory strategies in the management of OSCC.

The immune system plays a dual role in cancer—eliminating malignant cells while potentially promoting tumor escape under chronic stimulation. In OSCC, immune evasion is partly mediated through the PD-1/PD-L1 axis, an immune checkpoint pathway that suppresses T cell activation and fosters an immunosuppressive tumor microenvironment [20]. Elevated PD-L1 expression has been linked with poor prognosis and resistance to therapy, making it a target of interest in immunotherapy [21]. In parallel, the inflammasome represents a critical innate immune sensing mechanism, with the NLRP3 inflammasome being the most studied. The NLRP3 inflammasome is a critical component of the innate immune system that detects cellular damage and infections. The activated NLRP3 inflammasome is composed by the sensor protein NLRP3, the adaptor protein ASC (also known as PYCARD or TMS1), and the effector enzyme caspase-1, driving to the maturation and release of the pro-inflammatory cytokines IL-1 β and IL-18 [22]. Additionally, non-canonical routes linked to the NLRP3 inflammasome include caspase 5 and caspase 8, amplifying the responses initiated by the canonical pathway [23,24]. The hyperactivation of the NLRP3 inflammasome has been implicated in both tumor-promoting inflammation

and antitumor immunity, depending on the context [25,26]. Meanwhile, the sensor protein NAIP is critical for the activation of the NAIP-NLRC4 inflammasome, whose relevance in various types of cancer has been demonstrated in previous works [27]. Understanding how these pathways interact in OSCC could reveal critical mechanisms of immune regulation and suggest combinatory therapeutic approaches.

We hypothesize that the expression levels of inflammatory markers, particularly those related to the PD-1/PD-L1 axis along with the NLRP3 and NAIP inflammasome, are associated with specific clinical and pathological features of OSCC. The main objectives of this study are: (1) to assess the expression of PD-1, PD-L1, NLRP3, ASC/PYCARD, caspases, and IL-1 β /IL-18 in OSCC tissues; (2) correlate their expression profiles with critical clinical variables like sex, smoking, alcohol consumption, oral hygiene, tumor recurrence, vascular invasion, perineural invasion, ulceration, leukoplakia, tumor grade, and comorbidities, and (3) elucidate how these inflammatory pathways may drive disease progression and serve as prognostic or predictive biomarkers. By integrating detailed immunohistochemical analysis with rigorous statistical modeling, our work seeks to uncover mechanistic insights that could inform personalized prognostication and novel therapeutic strategies in oral cancer.

Patients and methods

Study design, sample processing

This is a retrospective observational study involving a cohort of 30 patients diagnosed with OSCC who underwent surgical resection. Data on relevant clinical variables were collected. All variables included in the analysis were complete, with no missing data.

OSCC samples were preserved in minimal essential medium (MEM; Thermo Fisher Scientific, Inc., Waltham, MA, USA) supplemented with 1% antibiotic/antimycotic (streptomycin, amphotericin B, and penicillin; Thermo Fisher Scientific, Inc.). The samples were processed under sterile conditions inside a class II laminar flow hood (Telstar AV 30/70 Müller 220 V 50 MHz; Telstar; Azbil Corporation, Chiyoda-ku, Tokyo, Japan). To eliminate erythrocytes, the MEM-preserved

samples were washed and rehydrated five times in antibiotic-free MEM. They were then cut into 2 cm sections using a clean scalpel and fixed in an F13 solution (composed of 60% ethanol, 20% methanol, 13% distilled water, and 7% polyethylene glycol), following established protocols. The samples were then embedded in paraffin molds, sectioned into 5 µm slices using an HM 350 S rotary microtome (Thermo Fisher Scientific, Inc., Waltham, MA, USA), and transferred onto glass slides treated with 10% poly-L-lysine after being placed in a warm water bath. These samples prepared were then used for histological analysis.

The study adhered to Good Clinical Practice guidelines, the principles outlined in the latest Declaration of Helsinki (2013), and the Oviedo Convention (1997). It was conducted in accordance with ethical principles such as autonomy, beneficence, non-maleficence, and distributive justice. Data collection followed current data protection regulations, including Regulation (EU) 2016/679 and Organic Law 3/5 of December 2018, which govern personal data protection and digital rights.

Immunohistochemistry

Paraffin-preserved oral tissue samples were analyzed using immunohistochemical techniques. The protocol details, including the antigen retrieval process, are outlined in **Table 1**. Antigen-antibody interactions were identified using the avid-

in-biotin complex (ABC) method in combination with avidin-peroxidase, following established protocols [28,29]. The samples were incubated overnight at 4°C with a 3% BSA blocker (Catalog #37525; Thermo Fisher Scientific, Inc., Waltham, MA, USA) and PBS after a 90-minute incubation with the primary antibody.

Next, the samples were incubated for 90 minutes at room temperature with a biotin-conjugated secondary antibody diluted in PBS: rabbit IgG (1/300, RG-96; Sigma-Aldrich, St. Louis, MO, USA), goat IgG (1/100, GT-34/B3148; Sigma-Aldrich), and mouse IgG (1/300, F2012/045K6072; Sigma-Aldrich). To enhance detection, ExtrAvidin®-Peroxidase (Sigma-Aldrich; Merck KGaA, Darmstadt, Germany), a conjugate of avidin and peroxidase, was applied for 60 minutes at room temperature (1:200 dilution in PBS).

Protein expression was visualized using a Chromogenic Diaminobenzidine (DAB) Substrate Kit (Cat. No. SK-4100; Maravai LifeSciences, San Diego, CA, USA), freshly prepared before use. The kit contained five milliliters of distilled water, two drops of buffer, four drops of DAB, and two drops of hydrogen peroxide. Protein presence was indicated by brown staining, as the chromogenic peroxidase substrate generated a signal within 15 minutes at room temperature. For each protein, tissue sections served as negative controls, where PBS replaced the primary antibody as the blocking solution. Carazzi hematoxylin was

Table 1. Primary and secondary antibodies used and their dilutions.

Antigen	Species	Dilution	Provider	Protocol Specifications
PD-1	Mouse Monoclonal	1/50	Abcam (ab234444)	-----
PD-L1	Rabbit monoclonal	1:500	Abcam (ab228415)	-----
NLRP3	Rabbit Monoclonal	1:500	Abcam (ab263899)	-----
ASC/ PYCARD	Rabbit monoclonal	1:250	Abcam (ab283684)	-----
Caspase 1	Rabbit Polyclonal	1:500	Abcam (ab62698)	-----
Caspase 5	Rabbit monoclonal	1:100	Abcam (ab40887)	-----
Caspase 8	Rabbit polyclonal	1:250	Abcam (ab25901)	-----
IL-1β	Rabbit recombinant multiclonal	1:50	Abcam (ab283818)	-----
IL-18	Rabbit monoclonal	1:50	Abcam (ab243091)	-----
NAIP	Rabbit Monoclonal	1:10	Abcam (ab25968)	-----
IgG (Rabbit)	Mouse	1:1000	Sigma-Aldrich (RG-96/B5283)	-----

Abbreviations: PD-1, programmed cell death protein 1; PD-L1, programmed death-ligand 1; NLRP3, NLR family pyrin domain containing 3; ASC/PYCARD, apoptosis-associated speck-like protein containing a CARD (PYD and CARD domain containing); IL-1β, interleukin-1 beta; IL-18, interleukin-18; NAIP, NLR family apoptosis inhibitory protein; IgG, immunoglobulin G.

used as a counterstain, with each tissue section incubated for 15 minutes at room temperature.

Histopathological analysis

Using an AxioCam HRc digital camera and a Zeiss Axiophot light microscope (Carl Zeiss, Oberkochen, Germany), tissue sections of each sample for the explored markers were observed by two independent pathologists. The interpretation of histological expression through Immunoreactivity scoring system (IRS) Scores obtained in this study is a codification in values 0, 1 and 2, being negative, low/moderate or high expression respectively, as defined in previous studies [30]

Statistical analysis

All analyses were performed using R software (version 4.1.3). Data management and statistical procedures made use of the following R packages: readxl for data import, dplyr for data manipulation, psych, Hmisc, and summarytools for descriptive and correlation analyses, ggplot2, reshape2, and gridExtra for visualization (including boxplots, violin plots, heatmaps, and correlograms), writexl and openxlsx for exporting results, flextable and officer for table formatting, and MASS for fitting ordinal logistic regression models. Formal citations for each package are collected in **Supplementary Material 1**.

Descriptive summary of the cohort

A descriptive analysis of the clinical and demographic characteristics of the cohort (n = 30) was generated using functions from summarytools, psych, and dplyr. Frequencies and percentages were reported for categorical variables, while mean and median were calculated for age.

Association between age and molecular markers expression

To explore potential relationships between patient age (continuous) and molecular marker expression levels (ordinal), Spearman's rank correlation coefficients were calculated using functions from *psych* and *Hmisc* in R. Spearman's method is non-parametric, does not assume normality, and captures monotonic associations based on ranked data. Correlation analysis was preferred over ordinal logistic regression because several markers did not meet the assumptions required for regression models, such as sufficient ordinal variability.

Association between groups (categorical variables) and markers expression

To investigate potential differences in molecular marker expression across clinical subgroups, we applied the Wilcoxon rank-sum test (also known as the Mann–Whitney U test) to each pairwise combination of binary categorical variables and molecular markers. The dataset included 11 categorical clinical features (*Sex, Smoking status, Alcohol consumption, Oral hygiene, Tumor recurrence, Vascular invasion, Perineural invasion, Ulceration, Leukoplakia, Tumor grade, and Comorbidity with systemic disease*), and 10 molecular markers (PD-L1, PD-1, NAIP, NLRP3, Caspase 1, Caspase 5, Caspase 8, IL-1 β , IL-18, PYCARD) measured on an ordinal scale (0–2). *Oral hygiene* was treated as a binary variable (good vs. poor) based on clinician-reported assessment in the medical records, reflecting whether patients were considered to have adequate oral hygiene habits and oral health at diagnosis. No standardized oral hygiene index was available.

For each variable-marker pair, participants were grouped based on the binary clinical variable (e.g., smoker vs. non-smoker), and the distributions of marker expression were compared. To ensure validity, only comparisons with more than one observation in both groups were retained.

Given the large number of pairwise tests conducted (11 variables \times 10 markers = 110 comparisons), p-values were adjusted using the Benjamini-Hochberg False Discovery Rate (FDR) procedure to control for the expected proportion of false positives. Associations were considered statistically significant at an adjusted p-value threshold of < 0.05 . This correction improves the reliability of the findings and mitigates the risk of type I errors due to multiple testing.

Molecular markers correlations through correlograms

Spearman correlation coefficients were computed using *Hmisc* to assess associations between pairs of molecular markers (ordinal scores 0–2). Heatmaps and correlograms were generated using *ggplot2*, *reshape2*, and *gridExtra*, visualizing both the magnitude and significance of correlations. We first made general heatmap to show the strength and signification of each pair of associations and corroborated the relationship of non-linearity through a scatterplot. Finally, we

stratified the cohort according to tumor grade to test if there were differences among co-expression patterns due to diverse disease manifestations.

Multivariable analysis: Binary Logistic Regression Models (BLRM)

Univariate and multivariable regression approaches serve different purposes: while multivariable models allow the simultaneous assessment of multiple predictors, univariate models are appropriate for exploratory analyses and for settings with limited sample size or high predictor interdependence.

An ordinal logistic regression model (OLRM) was initially explored using the `polr()` function from the MASS package in R to investigate factors associated with increasing levels of molecular marker expression, categorized on an ordinal scale (IRS scores: 0, 1, 2). Clinical and demographic variables were considered based on prior univariate analyses and biological plausibility. However, the OLRM showed convergence problems and unstable odds ratio estimates, likely due to sparse data within ordinal categories and the limited sample size.

Therefore, we adopted binary logistic regression models (BLRM) using the `glm()` function from the base stats package with a binomial family. Tumor grade was dichotomized (well differentiated vs. moderate/poorly differentiated), and each BLRM was specified as a univariate model, including a single molecular marker as the predictor. Odds ratios (ORs) and 95% confidence intervals (CIs) were obtained by exponentiating the regression coefficients. Statistical significance was defined as $p < 0.05$.

Although strong inter-marker correlations were observed in the correlograms—particularly within grade 2 tumors—multicollinearity was not formally assessed using variance inflation factors (VIF). This is because multicollinearity is mathematically impossible in univariate regression models, which contain only one predictor. Consequently, VIF calculations are not applicable in this analytical context.

The choice of univariate BLRM was driven by two considerations: (1) the limited sample size ($n = 30$), which would not support reliable multivariable estimation without substantial risk of overfitting, and (2) the high biological and statis-

tical interdependence among molecular markers, which would render multivariable models unstable and difficult to interpret.

Accordingly, all logistic regression analyses should be considered exploratory, and the observed associations warrant validation in larger, independent cohorts.

Results

Descriptive summary of the cohort

A descriptive summary of the cohort is presented in **Table 2**, detailing demographic, behavioral, clinical, and pathological characteristics of the 30 patients included in the study. The mean age was 73.9 years (± 9.9), with a median of 73 and an interquartile range (IQR) of 16.5. The sample had a balanced sex distribution, with 53.3% females and 46.7% males. A high proportion of patients reported smoking (90%), while 40% reported alcohol consumption. Regarding clinical features, 56.7% experienced tumor relapses, and 50% of tumors were classified as moderate/poorly differentiated. Notably, vascular invasion was present in 63.3% of cases, and perineural invasion in 36.7%. Additional relevant findings include ulceration in 73.3% of tumors, leukoplakia in 56.7% of patients, and the presence of systemic comorbidities in 40%. Good oral hygiene was observed in 53.3% of the cohort.

Patients with oral squamous cell carcinoma exhibit a differential expression of PD-1, PD-L1, NAIP and NLRP3 inflammasome-related markers

Then we assessed the histopathological expression of each marker, revealing that a subset of patients exhibited high levels of the different explored components (2); whereas others exhibit low/moderate (1) or even negative expression (0). In **table 3**, we summarize the percentage of patients identified according to each expression level. Meanwhile, in **figures 1–4** we represent histopathological images comparing high versus low/moderate expression for each marker

Association between age and molecular markers expression

We evaluated the association between patient age and the expression of 10 molecular markers

Table 2. Descriptive Summary of the Cohort.

Variable	Category/Value	Summary
Age		Mean 73.9 ± 9.9 – Median: 73 (IQR: 16.5)
Sex	Male	14 (46.7%)
	Female	16 (53.3%)
Smoker	No	3 (10%)
	Yes	27 (90%)
Drinker	No	18 (60%)
	Yes	12 (40%)
Good Oral Hygiene	No	14 (46.7%)
	Yes	16 (53.3%)
Relapse	No	13 (43.3%)
	Yes	17 (56.7%)
Tumor Grade	Moderate/Poorly differentiated or Grade 1	15 (50%)
	Well differentiated or Grade 2	15 (50%)
Vascular Invasion	No	11 (36.7%)
	Yes	19 (63.3%)
Perineural Invasion	No	19 (63.3%)
	Yes	11 (36.7%)
Ulcer	No	8 (26.7%)
	Yes	22 (73.3%)
Leukoplakia	No	13 (43.3%)
	Yes	17 (56.7%)
Comorbidity_Systemic_Disease	No	18 (60%)
	Yes	12 (40%)

Numerical variable Age expressed as mean +-SD and median with IQR (interquartile range). Categorical variables expressed as absolute frequencies and percentages.

Table 3. Expression level of the different biomarkers in our cohort of patients with OSCC.

Marker	High expression (2)	Low/moderate expression (1)	Negative expression (0)
PD-L1	17 (56.7%)	8 (26.7%)	5 (16.7%)
PD-1	16 (53.3%)	7 (23.3%)	7 (23.3%)
NAIP	18 (60.0%)	9 (30.0%)	3 (10.0%)
NLRP3	19 (63.3%)	8 (26.7%)	3 (10.0%)
CASPASE 1	20 (66.7%)	7 (23.3%)	3 (10.0%)
CASPASE 5	19 (63.3%)	8 (26.7%)	3 (10.0%)
CASPASE 8	18 (60.0%)	9 (30.0%)	3 (10.0%)
IL-1B	19 (63.3%)	8 (26.7%)	3 (10.0%)
IL-18	19 (63.3%)	9 (30.0%)	2 (6.7%)
PYCARD	16 (53.3%)	7 (23.3%)	7 (23.3%)

Abbreviations: PD-1, programmed cell death protein 1; PD-L1, programmed death-ligand 1; NLRP3, NLR family pyrin domain containing 3; ASC/PYCARD, apoptosis-associated speck-like protein containing a CARD (PYD and CARD domain containing); IL-1β, interleukin-1 beta; IL-18, interleukin-18; NAIP, NLR family apoptosis inhibitory protein.

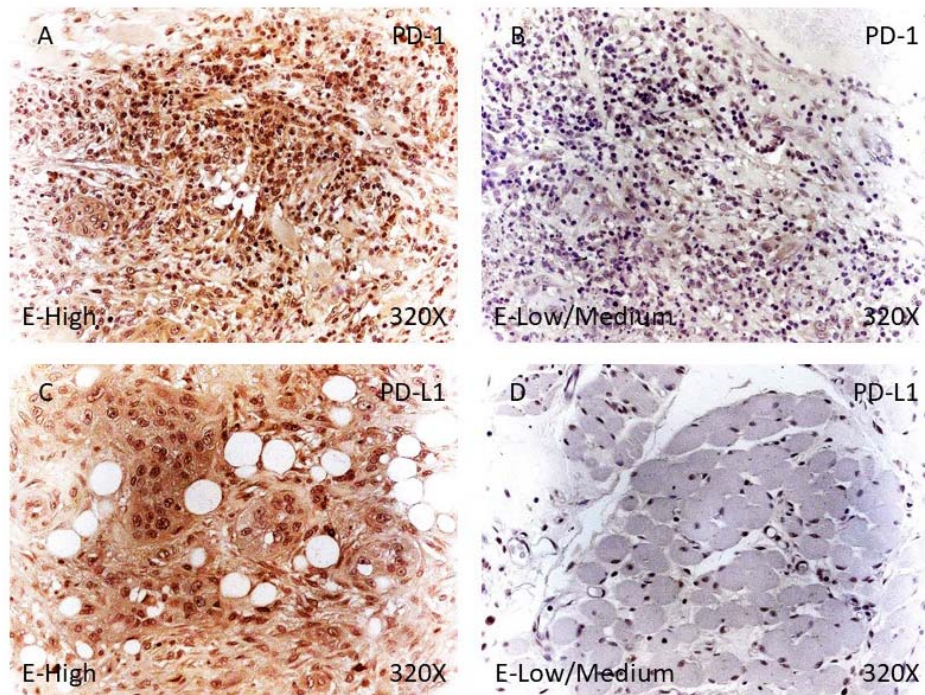


Figure 1. Representative images of high and low/medium expression levels for the markers PD-1 (A and B) and PD-L1 (C and D). Abbreviations: PD-1, programmed cell death protein 1; PD-L1, programmed death-ligand 1.

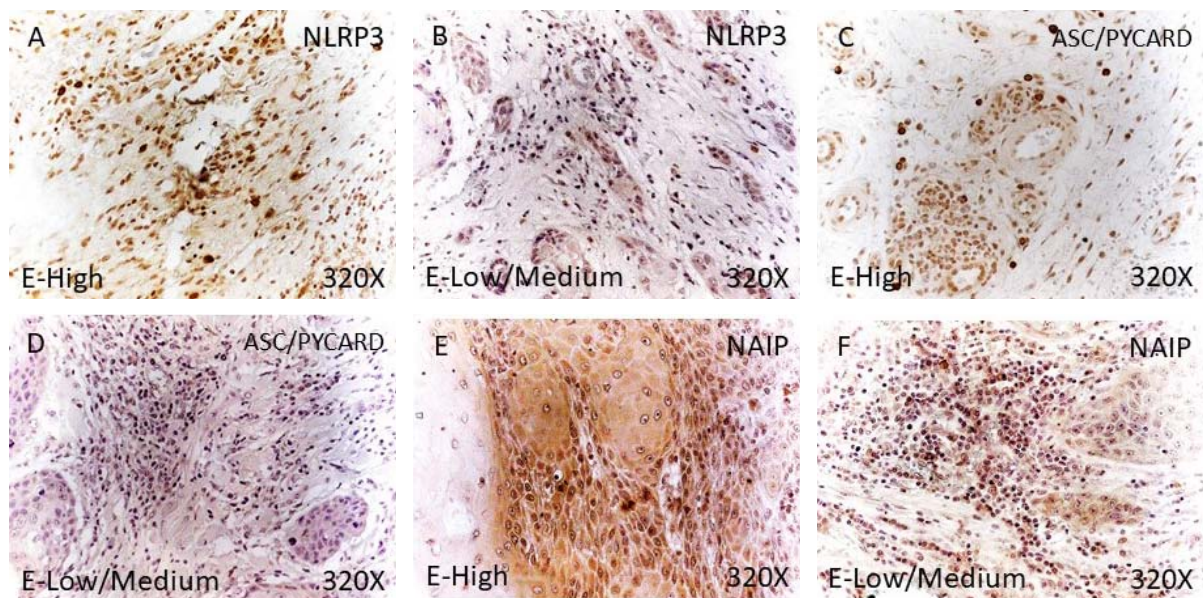


Figure 2. Representative images of high and low/medium expression levels for the markers NLRP3 (A and B), ASC/PYCARD (C and D) and NAIP (E and F). Abbreviations: NLRP3, NLR family pyrin domain containing 3; ASC/PYCARD, apoptosis-associated speck-like protein containing a CARD (PYD and CARD domain containing); NAIP, NLR family apoptosis inhibitory protein.

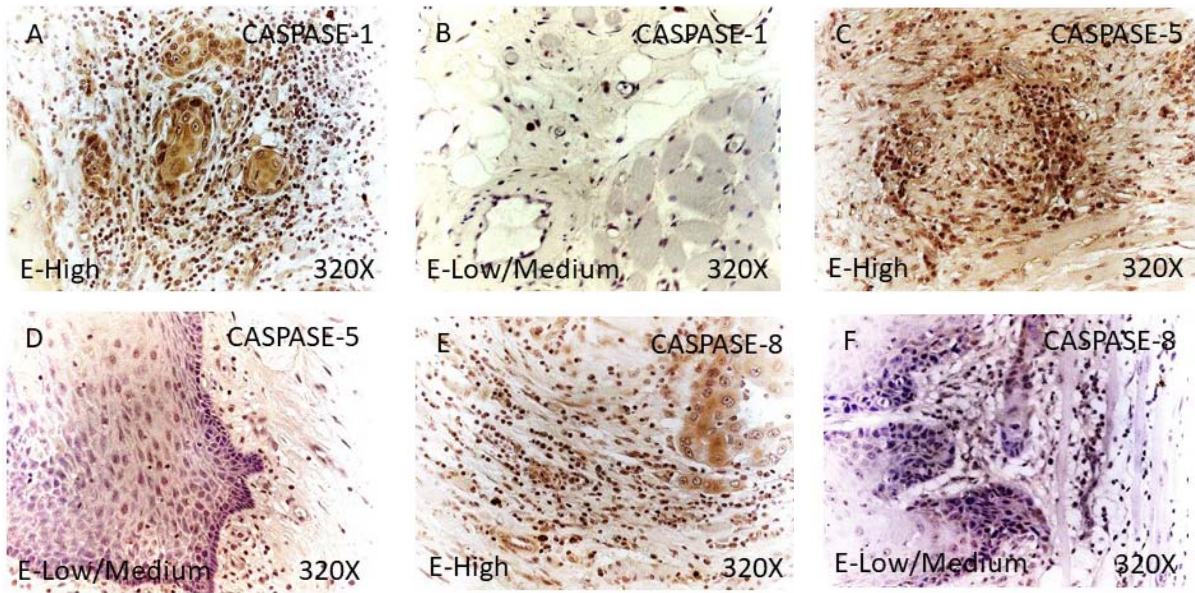


Figure 3. Representative images of high and low/medium expression levels for the markers caspase 1 (A and B), caspase 5 (C and D) and caspase 8 (E and F).

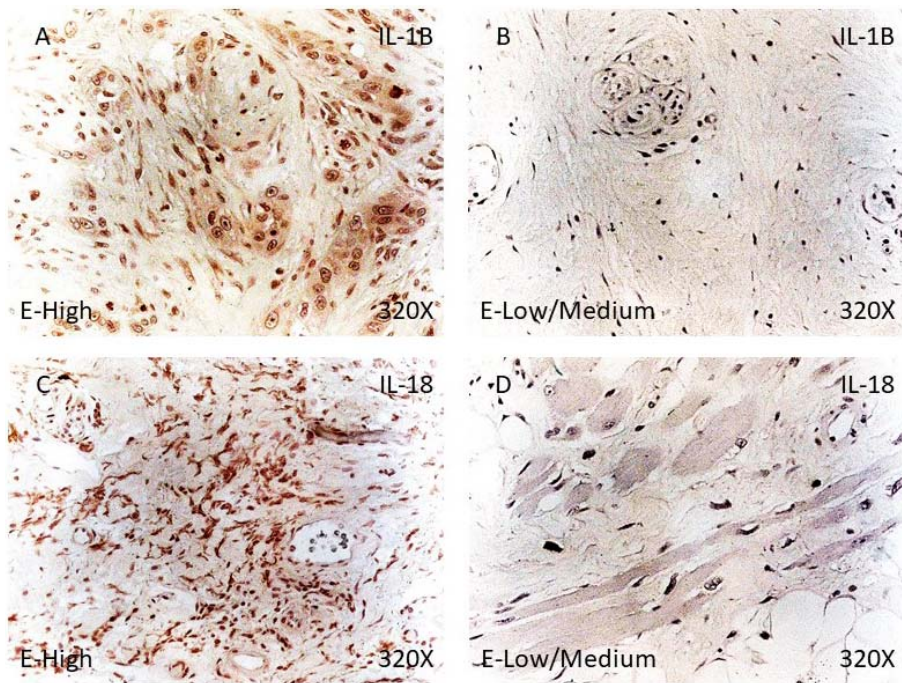


Figure 4. Representative images of high and low/medium expression levels for the markers IL-1 β (A and B) and IL-18 (C and D). Abbreviations: IL-1 β , interleukin-1 beta; IL-18, interleukin-18.

Table 4. Correlation table of age with molecular markers.

Marker	Spearman rho coefficient	Spearman p value
PD_L1	0.082	0.665
PD_1	0.081	0.669
NAIP	0.114	0.548
NLRP3	0.221	0.240
Caspase_1	0.026	0.891
Caspase_5	0.117	0.539
Caspase_8	0.161	0.394
IL_1B	-0.061	0.747
IL_18	-0.209	0.269
PYCARD	0.003	0.989

Abbreviations: PD-1, programmed cell death protein 1; PD-L1, programmed death-ligand 1; NLRP3, NLR family pyrin domain containing 3; ASC/PYCARD, apoptosis-associated speck-like protein containing a CARD (PYD and CARD domain containing); IL-1 β , interleukin-1 beta; IL-18, interleukin-18; NAIP, NLR family apoptosis inhibitory protein.

using Spearman's rank correlation. All correlation coefficients were low ($\rho < |0.22|$) and not statistically significant ($p > 0.05$), indicating no detectable monotonic relationship between age and marker expression (Table 4). Given these findings, ordinal logistic regression was not pursued.

Association between groups (categorical variables) and markers expression

Using the Wilcoxon rank-sum test, we found statistically significant differences in the expression levels of molecular markers when stratified by tumor grade, oral hygiene, relapse status, and vascular invasion (Table 5). Specifically, all 10 markers showed highly significant differences between tumor grades ($p < 0.001$). For oral hygiene, significant associations were observed for PD-L1, NAIP, Caspase-1, Caspase-8, IL-1B, and PYCARD ($p < 0.05$), and for PD-1 and Caspase-5 ($p < 0.01$). In the case of relapse, all markers were highly significant, $p < 0.001$, except Caspase-8, IL-1B, and IL-18, which reached significance at the $p < 0.01$ level. Regarding vascular invasion, PD-L1 showed a highly significant difference $p < 0.001$, while PD-1, NAIP, NLRP3, and IL-18 reached $p < 0.01$ significance, and Caspase-1, Caspase-5, IL-1B, and PYCARD showed differences at the $p < 0.05$ level.

In Supplementary materials, significant variable-marker associations may be visualized through boxplots, highlighting clinical factors that may influence biomarker expression patterns (Figures S1–S9).

Molecular markers correlations through correlograms

We performed first the general correlogram heatmap-like ($N = 30$) (Figure 5). A significant positive correlation was observed among all pairs of the 10 molecular markers evaluated, according to Spearman's correlation coefficient. All correlation values were positive, indicating that higher expression of one marker tends to be associated with higher expression of the others. Additionally, all pairs showed p -values < 0.001 , suggesting that these associations are statistically robust ($p < 0.001$ in all cases). This high intercorrelation could reflect shared molecular mechanisms or common inflammatory pathways activated in the analyzed tumors.

Biologically, the analyzed markers are mostly involved in immune and inflammatory signaling pathways, such as the PD-1/PD-L1 axis, associated with tumor immune evasion, and the NLRP3 inflammasome complex, related to the activation of inflammatory caspases (Caspase-1, Caspase-5) and the production of proinflammatory cytokines like IL-1 β and IL-18. This profile suggests a coordinated activation of innate immune response mechanisms and inflammatory processes associated with the tumor microenvironment.

We corroborated the non-linear relationships among molecular marker expressions through scatterplot visualizations, which illustrated consistent positive but non-linear associations between markers (Figure 6).

Table 5. Wilcox Test for categorical variables and FDR correction for p values.

Categorical Variable	Marker	p_value	FDR_p_value	Summary Significance
Tumor Grade	PD_L1	0.001	0.001	***
	PD_1	<0.001	<0.001	***
	NAIP	0.001	0.001	***
	NLRP3	<0.001	0.001	***
	Caspase_1	<0.001	<0.001	***
	Caspase_5	<0.001	<0.001	***
	Caspase_8	<0.001	0.001	***
	IL_1B	<0.001	<0.001	***
	IL_18	<0.001	<0.001	***
	PYCARD	<0.001	<0.001	***
Oral_Hygiene	PD_L1	0.010	0.034	*
	PD_1	0.002	0.008	**
	NAIP	0.007	0.025	*
	Caspase_1	0.008	0.029	*
	Caspase_5	0.001	0.007	**
	Caspase_8	0.003	0.013	*
	IL_1B	0.012	0.039	*
	PYCARD	0.003	0.015	*
Relapse	PD_L1	<0.001	<0.001	***
	PD_1	<0.001	<0.001	***
	NAIP	<0.001	<0.001	***
	NLRP3	<0.001	<0.001	***
	Caspase_1	<0.001	<0.001	***
	Caspase_5	<0.001	<0.001	***
	Caspase_8	0.002	0.009	**
	IL_1B	0.001	0.006	**
	IL_18	<0.001	0.003	**
	PYCARD	<0.001	<0.001	***
Vascular_Invasion	PD_L1	<0.001	0.001	***
	PD_1	<0.001	0.001	**
	NAIP	0.001	0.004	**
	NLRP3	<0.001	0.003	**
	Caspase_1	0.005	0.021	*
	Caspase_5	0.004	0.017	*
	IL_1B	0.004	0.017	*
	IL_18	0.001	0.005	**
	PYCARD	0.002	0.010	*

Only significant results are shown.

Abbreviations: PD-1, programmed cell death protein 1; PD-L1, programmed death-ligand 1; NLRP3, NLR family pyrin domain containing 3; ASC/PYCARD, apoptosis-associated speck-like protein containing a CARD (PYD and CARD domain containing); IL-1 β , interleukin-1 beta; IL-18, interleukin-18; NAIP, NLR family apoptosis inhibitory protein; FDR: False discovery rate.

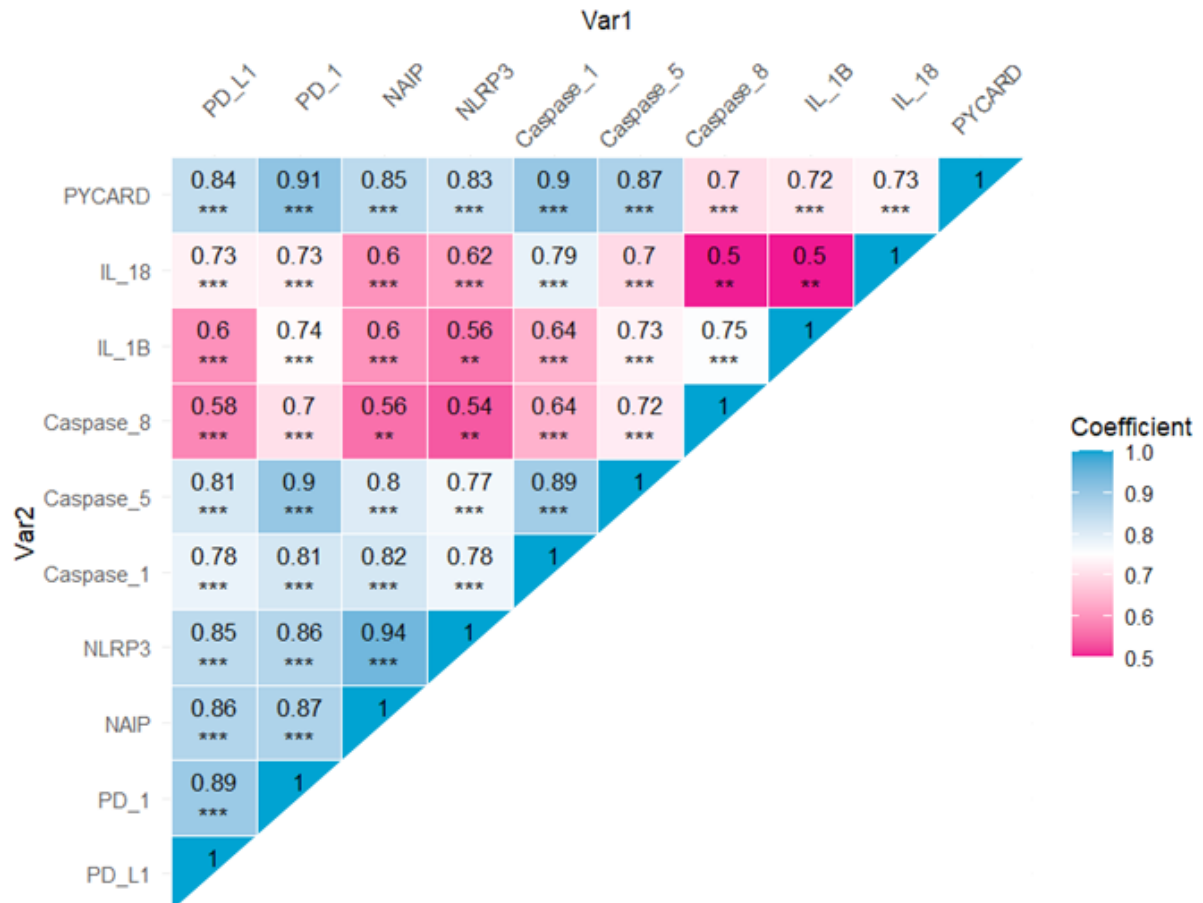


Figure 5. General Spearman correlation matrix. N = 30. Adjusted by FDR ($p < 0.05^*$, $p < 0.01^{**}$, $p < 0.001^{***}$). Abbreviations: PD-1, programmed cell death protein 1; PD-L1, programmed death-ligand 1; NLRP3, NLR family pyrin domain containing 3; ASC/PYCARD, apoptosis-associated speck-like protein containing a CARD (PYD and CARD domain containing); IL-1 β , interleukin-1 beta; IL-18, interleukin-18; NAIP, NLR family apoptosis inhibitory protein.

Since **Tumor Grade** was a significant variable in the Wilcoxon test, we also generated heatmaps stratified by Tumor Grade. This approach was used to identify whether the markers behave differently depending on the tumor grade. By visualizing the correlation matrices separately for each tumor grade, we aimed to explore if there are distinct patterns in the biological relationships between markers within each subgroup.

In the correlation heatmap for patients with Tumor Grade 1 (**Figure 7**, panel A), the variable *IL-1B* displayed no correlation values with any other markers, appearing as "NaN" (Not a Number) in the matrix. This is due to the lack of variability in *IL-1B* expression within this subgroup—all patients exhibited the same value. As correlation analysis relies on variation between values to detect patterns of association, a constant variable cannot produce meaningful correlation

coefficients. This suggests that *IL-1B* expression is uniformly distributed among Grade 1 tumors in our sample, and therefore, it does not contribute to inter-individual differences in this context. The same situation happened in the case of IL-18 for the correlation heatmap in Tumor Grade 2 (**Figure 7**, panel B).

Correlation heatmaps based on Spearman's coefficients revealed distinct co-expression profiles of the 10 molecular markers when stratified by tumor grade. In patients with **tumor grade 1** ($n = 15$), the range of Spearman's correlation coefficients extended from 0 to 1, suggesting a wide variability in marker associations. Statistically significant correlations were primarily moderate and selective. Notable associations included PD-L1 with PD-1 ($p < 0.001$), NLRP3 ($p < 0.05$), and PYCARD ($p < 0.05$); PD-1 with NAIP ($p < 0.01$) and NLRP3 ($p < 0.01$); and strong internal correlations

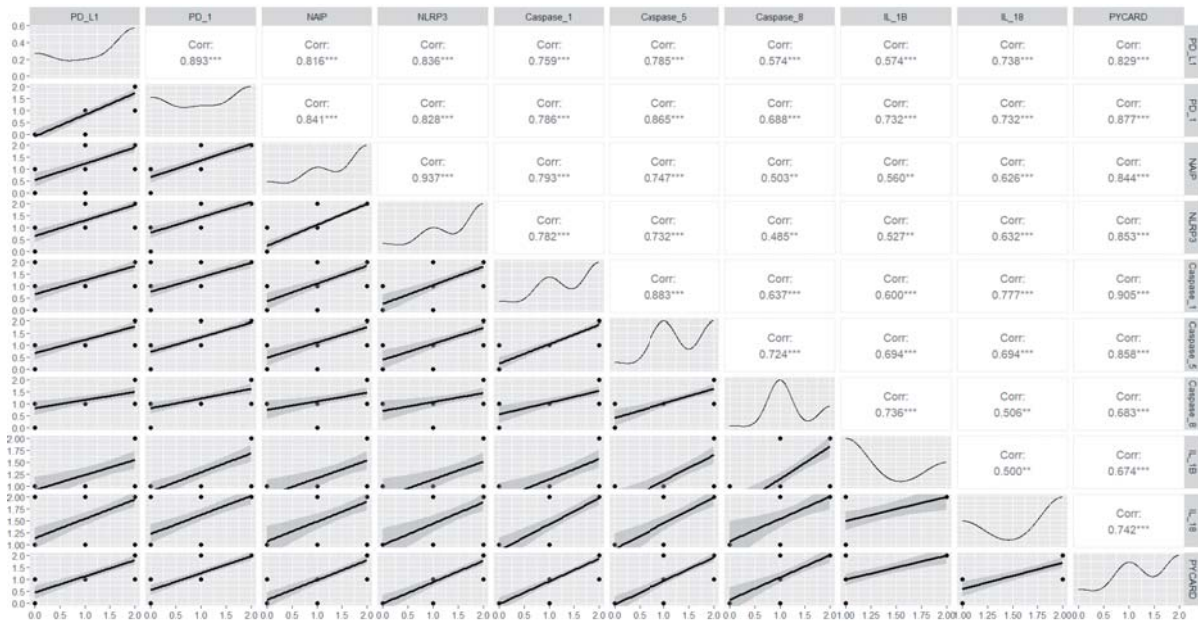


Figure 6. Pairwise Scatterplot evidences the non-linear relationship between each pair of molecular biomarkers. Abbreviations: PD-1, programmed cell death protein 1; PD-L1, programmed death-ligand 1; NLRP3, NLR family pyrin domain containing 3; ASC/PYCARD, apoptosis-associated speck-like protein containing a CARD (PYD and CARD domain containing); IL-1 β , interleukin-1 beta; IL-18, interleukin-18; NAIP, NLR family apoptosis inhibitory protein.

within the inflammasome axis, such as between Caspase-1 and NLRP3 ($p < 0.05$), Caspase-1 and IL-18 ($p < 0.05$), and Caspase-5 and Caspase-1 ($p < 0.05$). These findings suggest a relatively localized co-expression pattern among certain immune and inflammasome-related markers in lower-grade tumors (**Figure 7**, panel A).

In contrast, the heatmap for patients with **tumor grade 2** showed a substantial increase in co-expression, with Spearman coefficients ranging from **0.4 to 1**, and a marked abundance of strong or perfect correlations ($\rho = 1$) between most marker pairs. Almost all correlations in this group were statistically significant at the $p < 0.001$ level, indicating a more integrated or synchronized expression profile in higher-grade tumors. Exceptions included slightly weaker correlations such as PYCARD-NLRP3 ($p < 0.01$), PYCARD-IL1B ($p < 0.05$), and NLRP3 with IL1B, which did not reach significance. Notably, IL-1B showed significant but less intense correlations with most markers ($p < 0.05$), excluding IL-18 (which was not available for analysis) and NLRP3 (non-significant). These patterns suggest a possible network activation or transcriptional coordination among immune and inflammasome-related

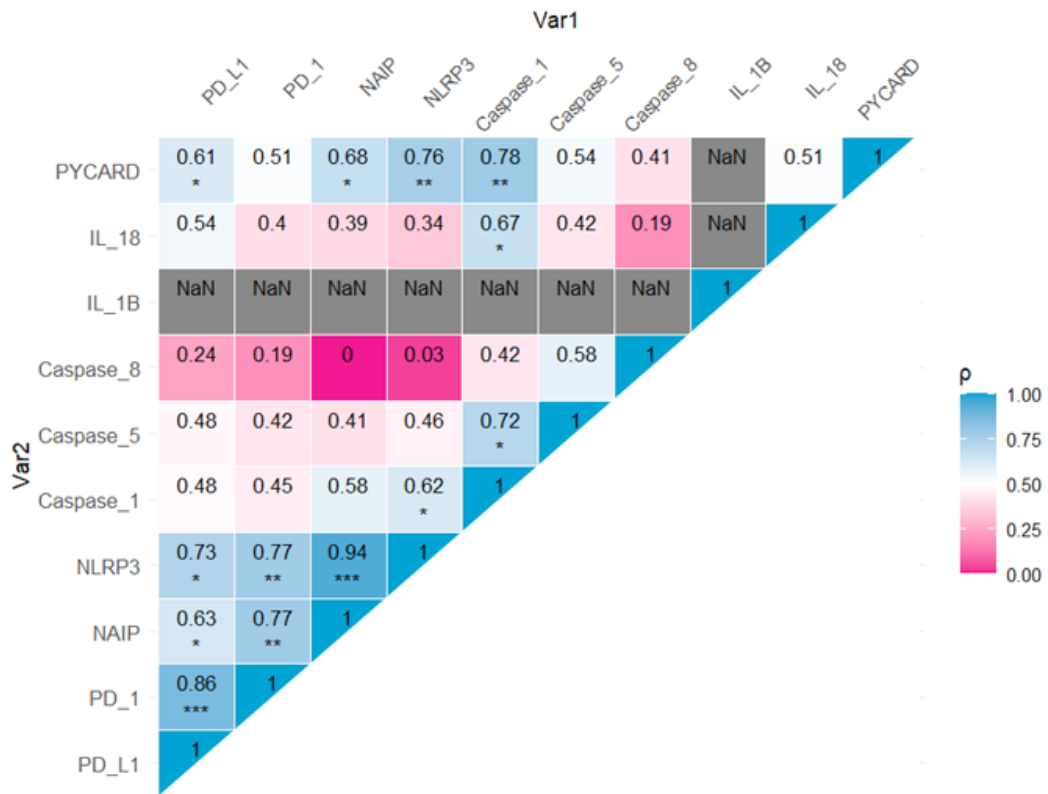
pathways as tumor aggressiveness increases (**Figure 7**, panel B).

While correlation heatmaps provide valuable insights into potential co-expression patterns and pathway coordination, their interpretive value is limited by sample size, especially in subgroup analyses (e.g., $n = 15$ for grade 1 tumors). Additionally, the presence of "perfect" correlations ($\rho = 1$) in tumor grade 2 may reflect overfitting or collinearity driven by small group size or low variability, rather than true biological relationships. Spearman's coefficients capture only monotonic relationships and do not imply causality. Furthermore, missing data (e.g., IL-18 correlations) and the inability to adjust for confounding variables in heatmap representations restrict the conclusions to descriptive levels. Therefore, findings from these visualizations should be interpreted cautiously and ideally confirmed through multivariate modeling or experimental validation.

Multivariable analysis: Binary Logistic Regression Models (BLRM)

Binary logistic regression models (BLRM) were used to evaluate the association between the expression levels of individual molecular mark-

A



B

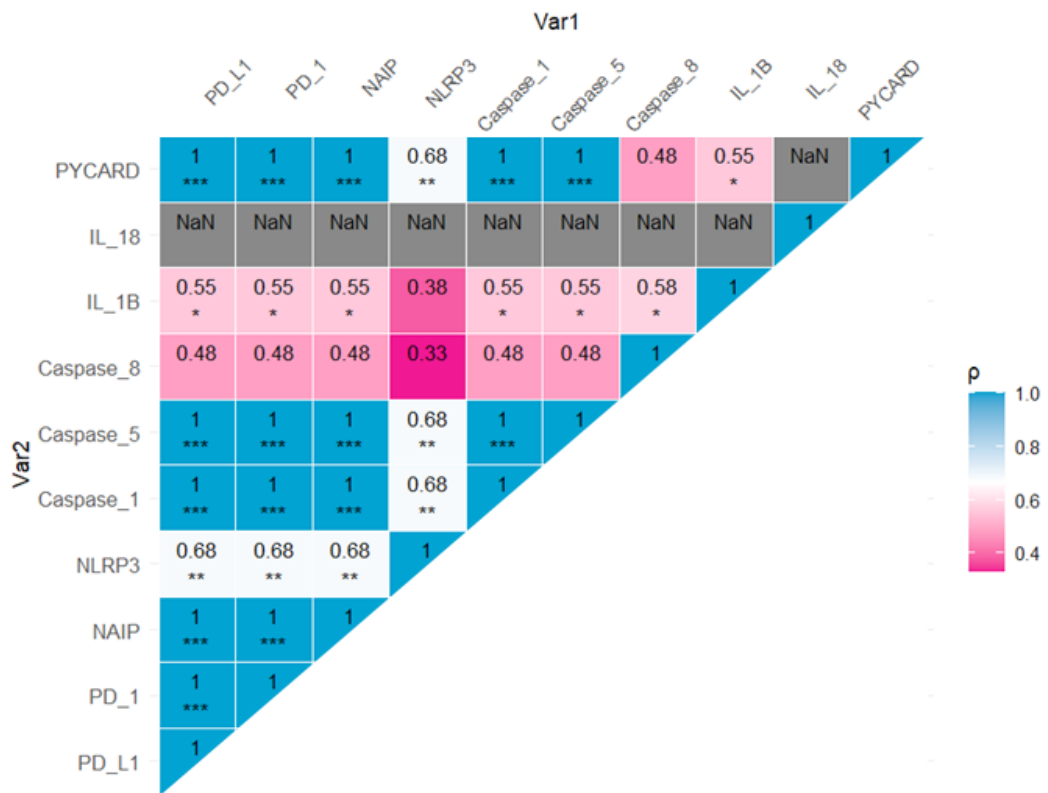


Figure 7. A. Tumor grade 1. N = 15. Adjusted by FDR ($p < 0.05^*$, $p < 0.01^{**}$, $p < 0.001^{***}$). B. Tumor Grade 2. N = 15. Adjusted by FDR. ($p < 0.05^*$, $p < 0.01^{**}$, $p < 0.001^{***}$). Abbreviations: PD-1, programmed cell death protein 1; PD-L1, programmed death-ligand 1; NLRP3, NLR family pyrin domain containing 3; ASC/PYCARD, apoptosis-associated speck-like protein containing a CARD (PYD and CARD domain containing); IL-1 β , interleukin-1 beta; IL-18, interleukin-18; NAIP, NLR family apoptosis inhibitory protein.

ers (IRS scores 0–2) and tumor grade (Grade 1 vs. Grade 2). The models estimate the odds of presenting with Grade 2 tumors relative to Grade 1, with odds ratios (ORs) greater than 1 indicating a positive association with higher tumor grade.

As shown in **Table 6**, higher expression levels of several markers were significantly associated with increased odds of Grade 2 tumors, including PD-L1 (OR: 9.46; 95% CI: 2.63–67.83; $p = 0.005$), NAIP (OR: 12.94; 95% CI: 2.79–107.66; $p = 0.005$), NLRP3 (OR: 28.93; 95% CI: 4.25–618.02; $p = 0.004$), Caspase-1 (OR: 20.52; 95% CI: 3.80–190.81; $p = 0.002$), Caspase-5 (OR: 78.74; 95% CI: 9.32–1955.60; $p = 0.001$), and PYCARD (OR: 66.78; 95% CI: 8.17–1655.40; $p = 0.001$).

In contrast, PD-1, Caspase-8, IL-1 β , and IL-18 did not show statistically significant associations with tumor grade ($p > 0.99$). For these markers, extremely large OR estimates with undefined or infinite confidence intervals reflect numerical instability due to sparse data and quasi-complete separation rather than reliable biological effects (**Table 6**).

Odds ratios (ORs) indicate the likelihood of presenting with moderate/poorly differentiated tumors versus well-differentiated tumors associated with higher molecular marker expression (IRS score 0–2). Confidence intervals (CI) correspond to 95% limits. Extremely large ORs with undefined upper confidence bounds reflect numerical instability due to sparse data rather

than true biological effects. For some markers, confidence intervals could not be fully estimated (upper bound = NA), reflecting numerical instability due to sparse data and quasi-complete separation rather than true infinite effect sizes.

OR (Odds Ratio) indicates the likelihood of presenting with tumor grade 2 (versus grade 1) associated with higher expression of the corresponding marker. An OR greater than 1 suggests a positive association. If $OR > 1$, higher expression of the marker is associated with greater odds of having Grade 2 (i.e., more aggressive tumors). If $OR < 1$, higher expression is associated with greater odds of being Grade 1 (i.e., less aggressive tumors). CI_{inf} and CI_{sup} represent the lower and upper bounds of the 95% confidence interval for the OR, respectively; narrower intervals reflect greater estimate precision. A p -value < 0.05 was considered statistically significant.

BLRM were conducted to evaluate the association between molecular marker expression and disease relapse. Among the markers analyzed, NAIP (OR = 129.64; 95% CI: 7.29–2306.77; $p = <0.0019$), NLRP3 (OR = 65.04; 95% CI: 5.22–810.03; $p = 0.0012$), Caspase-1 (OR = 68.99; 95% CI: 5.60–850.77; $p = 0.001$), and IL-18 (OR = 36.00; 95% CI: 3.47–373.14; $p = 0.0027$) showed statistically significant positive associations with relapse, suggesting that higher expression of these markers may be linked to increased likelihood of disease recurrence. In contrast, other

Table 6. Binary Logistic Regression Models Assessing the Association Between Tumor Grade and Molecular Marker Expression (Sensitivity Analysis).

Marker	Tumor Grade			P_value
	OR	CI_inf	CI_sup	
PD_L1	9.46	2.63	67.83	0.005
PD_1	3.4E+09	0	Inf	0.997
NAIP	12.942	2.79	107.66	0.005
NLRP3	28.927	4.25	618.02	0.004
Caspase_1	20.521	3.80	190.81	0.002
Caspase_5	78.741	9.32	1955.60	0.001
Caspase_8	6.34E+08	0	Inf	0.995
IL_1B	9.43E+08	0	Inf	0.995
IL_18	9.43E+08	0	Inf	0.995
PYCARD	66.776	8.17	1655.40	0.001

Abbreviations: PD-1, programmed cell death protein 1; PD-L1, programmed death-ligand 1; NLRP3, NLR family pyrin domain containing 3; ASC/PYCARD, apoptosis-associated speck-like protein containing a CARD (PYD and CARD domain containing); IL-1 β , interleukin-1 beta; IL-18, interleukin-18; NAIP, NLR family apoptosis inhibitory protein; OR, odds ratio; CI_{inf}, Confidence interval inferior; CI_{sup}, Confidence interval superior.

markers such as PD-L1, PD-1, Caspase-5, Caspase-8, IL-1B, and PYCARD did not reach statistical significance, likely due to wide or undefined confidence intervals and limited data variability. These findings highlight a potential inflammatory and pyroptotic signature associated with relapse in oral cancer (Table 7).

BLRM analysis revealed that poorer oral hygiene was significantly associated with higher expression of several inflammatory and pyroptosis-related markers. Specifically, PD-L1 (OR = 0.292; 95% CI: 0.101–0.846; p = 0.0234), PD-1 (OR = 0.189; 95% CI: 0.060–0.596;

p = 0.0045), NAIP (OR = 0.191; 95% CI: 0.046–0.796; p = 0.0229), NLRP3 (OR = 0.232; 95% CI: 0.056–0.962; p = 0.0441), Caspase-1 (OR = 0.144; 95% CI: 0.031–0.675; p = 0.0139), Caspase-5 (OR = 0.071; 95% CI: 0.012–0.411; p = 0.0032), Caspase-8 (OR = 0.052; 95% CI: 0.005–0.497; p = 0.0103), IL-1B (OR = 0.107; 95% CI: 0.017–0.662; p = 0.0162), and PYCARD (OR = 0.153; 95% CI: 0.036–0.656; p = 0.0115) all showed statistically significant inverse associations with oral hygiene status. These ORs below 1 indicate that individuals with poor oral hygiene were more likely to express higher levels of these markers. IL-18,

Table 7. Binary Logistic Regression Models Assessing the Association Between Relapse and Molecular Marker Expression.

Marker	Relapse			
	OR	CI_inf	CI_sup	P_value
PD_L1	8.14E+21	0	Inf	1
PD_1	8.49E+08	0	Inf	1
NAIP	129.635	7.285	2306.769	0.001
NLRP3	65.035	5.222	810.033	0.001
Caspase_1	68.993	5.595	850.771	0.001
Caspase_5	2.52E+09	0	Inf	0.996
Caspase_8	4.38E+08	0	Inf	0.995
IL_1B	5.84E+08	0	Inf	0.995
IL_18	36	3.473	373.137	0.003
PYCARD	1.88E+09	0	Inf	0.996

Abbreviations: PD-1, programmed cell death protein 1; PD-L1, programmed death-ligand 1; NLRP3, NLR family pyrin domain containing 3; ASC/PYCARD, apoptosis-associated speck-like protein containing a CARD (PYD and CARD domain containing); IL-1 β , interleukin-1 beta; IL-18, interleukin-18; NAIP, NLR family apoptosis inhibitory protein; OR, odds ratio; CI_inf. Confidence interval inferior; CI_sup: Confidence interval superior.

Table 8. Binary Logistic Regression Models Assessing the Association Between Oral Hygiene and Molecular Marker Expression.

Marker	Oral Hygiene			
	OR	CI_inf	CI_sup	P_value
PD_L1	0.292	0.101	0.846	0.023
PD_1	0.189	0.06	0.596	0.005
NAIP	0.191	0.046	0.796	0.023
NLRP3	0.232	0.056	0.962	0.044
Caspase_1	0.144	0.031	0.675	0.014
Caspase_5	0.071	0.012	0.411	0.003
Caspase_8	0.052	0.005	0.497	0.0103
IL_1B	0.107	0.017	0.662	0.016
IL_18	0.351	0.07	1.761	0.203
PYCARD	0.153	0.036	0.656	0.012

Abbreviations: PD-1, programmed cell death protein 1; PD-L1, programmed death-ligand 1; NLRP3, NLR family pyrin domain containing 3; ASC/PYCARD, apoptosis-associated speck-like protein containing a CARD (PYD and CARD domain containing); IL-1 β , interleukin-1 beta; IL-18, interleukin-18; NAIP, NLR family apoptosis inhibitory protein; OR, odds ratio; CI_inf. Confidence interval inferior; CI_sup: Confidence interval superior.

while displaying a similar trend (OR = 0.351), did not reach statistical significance ($p = 0.2032$). These results suggest that poor oral hygiene may contribute to an upregulation of immune and inflammatory signaling pathways relevant to tumor behavior. On the contrary, where better oral hygiene may correspond to lower expression of key immune and pyroptosis markers (**Table 8**).

BLRM analysis demonstrated that the presence of vascular invasion was significantly associated with increased expression of multiple immune and inflammasome-related markers. Strong positive associations were observed for PD-L1 (OR = 11.213; 95% CI: 2.536–49.579; $p = 0.0014$), PD-1 (OR = 12.435; 95% CI: 2.502–61.803; $p = 0.0021$), NAIP (OR = 12.667; 95% CI: 2.256–71.114; $p = 0.0039$), NLRP3 (OR = 18.025; 95% CI: 2.705–120.094; $p = 0.0028$), IL-18 (OR = 22.667; 95% CI: 3.140–163.635; $p = 0.002$), and PYCARD (OR = 7.886; 95% CI: 1.661–37.429; $p = 0.0094$). Caspase-1 (OR = 5.768; $p = 0.016$) and Caspase-5 (OR = 7.669; $p = 0.0164$) were also significantly associated with vascular invasion, though with slightly wider confidence intervals. Caspase-8 (OR = 3.213; $p = 0.1708$) did not reach statistical significance, and IL-1B presented computational instability (OR $\approx 3.84 \times 10^8$; CI: 0–Inf; $p = 0.9954$), suggesting unreliable estimation. These findings suggest a strong relationship between vascular invasion and elevated expression of specific pro-inflammatory and immune checkpoint markers (**Table 9**).

Discussion

In the present work, we identified significant associations between key clinical variables in patients with OSCC—including tumor grade, relapse, vascular invasion, and oral hygiene—and the histopathological expression of PD-1 and PD-L1, along with several markers involved in both canonical and non-canonical NLRP3 inflammasome pathways. These included NLRP3, the adaptor protein PYCARD, caspases 1, 5, and 8, the cytokines IL-1 β and IL-18, as well as NAIP, a key sensor protein of the NAIP/NLRC4 inflammasome. Notably, our findings suggest a coordinated upregulation of inflammasome components and immune checkpoint markers in higher-grade tumors, relapsing cases, and those with vascular invasion. In contrast, oral hygiene was inversely associated with these same markers. Coordinately, these patterns support the hypothesis of a pro-inflammatory microenvironment linked to tumor progression and immune modulation. Conversely, other commonly considered clinical factors such as sex, smoking, alcohol consumption, perineural invasion, ulceration, leukoplakia, and systemic comorbidities did not show statistically significant associations with marker expression. Herein, we will contextualize these findings in light of current literature, discussing their biological relevance and potential implications, while acknowledging the methodological strengths and limitations of our study.

Table 9. Binary Logistic Regression Models Assessing the Association Between Vascular Invasion and Molecular Marker Expression.

Marker	Vascular Invasion			
	OR	CI_inf	CI_sup	P_value
PD_L1	11.213	2.536	49.579	0.001
PD_1	12.435	2.502	61.803	0.002
NAIP	12.667	2.256	71.114	0.004
NLRP3	18.025	2.705	120.094	0.003
Caspase_1	5.768	1.387	23.993	0.016
Caspase_5	7.669	1.452	40.508	0.016
Caspase_8	3.213	0.605	17.069	0.171
IL_1B	3.84E+08	0	Inf	0.995
IL_18	22.667	3.14	163.635	0.002
PYCARD	7.886	1.661	37.429	0.009

Abbreviations: PD-1, programmed cell death protein 1; PD-L1, programmed death-ligand 1; NLRP3, NLR family pyrin domain containing 3; ASC/PYCARD, apoptosis-associated speck-like protein containing a CARD (PYD and CARD domain containing); IL-1 β , interleukin-1 beta; IL-18, interleukin-18; NAIP, NLR family apoptosis inhibitory protein; OR, odds ratio; CI_inf. Confidence interval inferior; CI_sup: Confidence interval superior.

PD-1 and PDL-1

The PD-1/PD-L1 axis is a key immune checkpoint pathway that regulates T cell activation and maintains peripheral tolerance [20, 31,32]. PD-1, expressed on activated T and B cells, contains cytoplasmic inhibitory motifs (ITIM and ITSM) that, upon binding to PD-L1, recruit SHP-2 phosphatases. This interaction inhibits critical signaling pathways such as PI3K/AKT, MAPK/ERK, and JAK/STAT, leading to reduced cytokine production, T cell proliferation, and immune responses. PD-L1, expressed on tumor cells and antigen-presenting cells, is upregulated by inflammatory stimuli like IFN- γ via the JAK/STAT and NF- κ B pathways. In cancer, PD-L1 contributes to immune evasion by promoting T cell exhaustion and also drives tumor progression through cell-intrinsic signaling, including epithelial-to-mesenchymal transition and enhanced survival [20]. Together, PD-1/PD-L1 help tumors escape immune surveillance, making them crucial targets in cancer immunotherapy.

PD-1 and PDL-1 are two well-established biomarkers in different types of cancer, including OSCC [33]. The association with higher tumor grade and relapse aligns with previous studies indicating that upregulation of PD-1/PDL1 is linked to more aggressive and immune-resistant tumor phenotypes, with critical functions in OSCC carcinogenesis [34, 35] Furthermore, the correlation with vascular invasion suggests that PD-1/PD-L1 expression may also contribute to tumor dissemination mechanisms, possibly by creating an immunosuppressive milieu that facilitates tumor progression and intravasation, as supported in past works [36] Contrary to our results, other works [37] found that vascular invasion showed a trend toward lower PD-L1. Despite this, current literature shows inconclusive and mixed results regarding the possible prognostic role of PD-1/PD-L1 in OSCC [21,33,38].

Interestingly, poor oral hygiene, a modifiable environmental factor, was also associated with elevated expression of PD-1/PD-L1. Poor oral hygiene strongly favors the expansion of pathogenic oral microbiota which may contribute to OSCC development and progression by prompting inflammatory responses and modulating tumor microenvironment [39,40]. As some studies have reported some specific changes in gut microbiota between PD-1/PD-L1 positive

and PD-1/PD-L1 negative patients [41], it will be interesting to deepen on the possible role of oral microbiota in the dysregulation of PD-1/PD-L1, especially in case of advanced tumors. For example, *Porphyromonas gingivalis* cell wall components have been shown to induce PD-L1 expression on human oral carcinoma cells [42], providing a direct mechanistic link between periodontal pathogens (common in poor hygiene) and checkpoint upregulation.

In contrast, other commonly studied clinical factors such as sex, tobacco and alcohol use, or perineural invasion did not correlate with PD-1/PD-L1 expression in our cohort. Available literature is quite heterogeneous in terms of these associations. For instance, a prior meta-analysis performed by [43] reported that PD-1/PD-L1 expression was correlated with sex, metastasis, low differentiation and HPV infection, but not with TNM or T stage. On the other hand, other works found that tumor size, pattern, depth of invasion lymphovascular invasion, and perineural invasion were significantly associated with PD-L1 immunohistochemical scores [44]. Sex, metastasis and smoking was also correlated with PD-L1 in other works [38]. On the contrary, other works [45] showed that never smokers and never drinkers tend to exhibit heightened PD-1/PD-L1 signaling. Leukoplakia, another non-significant clinical variable included in our work, was also associated with higher PD-L1 levels [46].

Overall, the relationship between clinical variables and the histopathological expression of PD-1 and PD-L1 in OSCC appears to be multifactorial and highly dependent on the biological context of each tumor and patient. While our findings support a strong association of PD-1/PD-L1 with more aggressive clinical features—such as higher tumor grade, relapse, and vascular invasion—literature reports on this topic remain mixed and sometimes contradictory, reflecting the complexity of these immune checkpoints in OSCC pathophysiology. Notably, the association we observed with poor oral hygiene adds a novel layer to this discussion, potentially linking local inflammatory states and oral dysbiosis to immune checkpoint regulation and tumor progression. On the other hand, the absence of correlation with other frequently studied variables, such as sex, tobacco or alcohol use, or perineural invasion, is consistent with the heterogeneity

found in prior studies and meta-analyses. Altogether, our results underscore the relevance of PD-1 and PD-L1 not only as markers of immune escape but also as potential indicators of tumor aggressiveness and inflammation-driven modulation. This highlights their utility as prognostic tools and strengthens the rationale for their therapeutic targeting in carefully selected OSCC patient subgroups.

NLRP3 and NAIP inflammasome

The NLRP3 inflammasome is a key component of the innate immune system, triggered through a tightly regulated two-step process: priming and activation. During the priming phase, pathogen- or damage-associated molecular patterns (PAMPs/DAMPs) activate pattern recognition receptors (PRRs), leading to NF- κ B signaling and subsequent transcriptional upregulation of NLRP3, pro-caspase-1, pro-IL-1 β , and to a lesser extent IL-18, which is constitutively expressed [22]. In the activation step, a wide range of cellular stress signals—including potassium efflux, mitochondrial dysfunction, and reactive oxygen species (ROS) production—trigger the oligomerization of NLRP3 [47]. This promotes the recruitment of the adaptor protein ASC/PYCARD, which in turn facilitates the autocatalytic activation of caspase-1. Active caspase-1 cleaves pro-IL-1 β and pro-IL-18 into their mature, bioactive forms, along with gasdermin D (GSDMD), responsible for forming a transmembrane pore that facilitates the secretion of active IL-1 β and IL-18, which are then secreted to mediate strong pro-inflammatory responses and a special type of cell death known as pyroptosis [48,49]. Other caspases such as caspase-5 and caspase-8 can also trigger pyroptosis via non-canonical NLRP3 inflammasome pathways [50]. Caspase-5 responds to PAMPs and DAMPs by either cleaving GSDMD to induce pyroptotic cell death or activating the NLRP3 inflammasome, leading to IL-1 β and IL-18 production. Meanwhile, caspase-8, typically activated by death receptors (e.g., FAS, TNF-R), can regulate IL-1 β expression both independently and through inflammasome modulation, depending on the stimulus [51].

The NAIP/NLRC4 inflammasome is a protein complex that detects bacterial components like flagellin and initiates immune responses. NAIPs recognize specific ligands using their NBD

domain and, upon binding, relieve their auto-inhibited state. This allows them to activate NLRC4 by exposing interaction surfaces that promote NLRC4 oligomerization. Once assembled, the inflammasome recruits and activates caspase-1 via NLRC4's CARD domain, leading to the cleavage of pro-inflammatory cytokines (IL-1 β , IL-18) and gasdermin D (GSDMD), triggering pyroptosis. NAIPs act as initiators, and each complex typically contains one NAIP and 9–11 NLRC4 units [52].

Our findings demonstrate a significant correlation between several clinical variables – namely tumor grade, relapse, vascular invasion, and poor oral hygiene – and the histopathological expression of key components of the NLRP3 inflammasome in OSCC, including NLRP3, ASC/PYCARD, caspase-1, IL-1 β , and IL-18, as well as non-canonical effectors caspase-5 and caspase-8 (with some exceptions like the lack of association between caspase 8 and vascular invasion or NLRP3 and IL-18 with oral hygiene). In agreement with our observations, Wang et al. [53] observed that NLRP3 was aberrantly overexpressed in OSCC cells, and also that the abnormal expression was correlated with the tumor stage, lymph node metastatic status and IL-1 β expression level. Similarly, increased expression of NLRP3 and IL-1 β in potentially malignant oral disorders correlates with higher transformation rates, along with tumor progression and dedifferentiation in OSCC [54]. It was also reported that the NLRP3 inflammasome-related proteins, NLRP3, PYCARD, caspase 1 and IL-1 β , were all highly expressed in OSCC tumor cells compared to adjacent normal cells [55]. Of them, they observed that PYCARD was significantly associated with tumor stage, node stage, overall stage, extracapsular spread, perineural invasion and tumor depth, also acting as a marker of poor prognosis in this type of tumors. Caspase 1 was seen to be correlated with nodal stage, overall clinical stage, and perineural invasion in OSCC, whereas high expression of IL-1 β was correlated with age and overall stage [55]. IL-18 expression in OSCC tissues has been linked to tumor differentiation. Interestingly, while IL-18 overexpression promoted tumor cell migration and invasion in vitro, it inhibited tumor growth in xenograft models, suggesting a complex role in tumor biology [56]. These studies highlight the involvement

of canonical NLRP3 inflammasome components in OSCC progression and their potential as biomarkers for tumor aggressiveness. However, inflammasome signaling is highly context-dependent, with both tumor-promoting and suppressive effects reported. For example, NLRP3-driven IL-1 β /IL-18 signaling often promotes proliferation, invasion and an immunosuppressive microenvironment in many cancers whereas in other settings inflammasome-induced pyroptosis or IL-18 release can inhibit tumor growth (as seen in colitis-associated cancers) [25]. Indeed, blocking IL-1 β or IL-18 has been shown to reduce tumor growth, while paradoxically inhibiting NLRP3 itself can sometimes enhance it [25]. This dual nature implies that our observation of elevated inflammasome markers in aggressive OSCC likely reflects a protumoral role under these specific conditions; although further studies are needed in order to understand the context-dependent role of NLRP3 inflammasome in cancer.

Moreover, the elevated presence of caspase-5 and caspase-8 in association with more aggressive clinical features highlights the involvement of non-canonical pathways. For instance, Liu et al. [57] described that caspase-8 is significantly overexpressed in OSCC tumor tissues compared to adjacent normal tissues, reporting that this overexpression was correlated with lymph node invasion, suggesting a role in tumor progression. Other studies [58,59] have also found that mutations in the CASP8 gene are present in approximately 10% of head and neck squamous cell carcinoma cases. These mutations are associated with resistance to death receptor-mediated apoptosis, necroptosis, enhanced cellular migration and invasion, and increased tumor growth, claiming that patients with CASP8 mutations tend to have a poorer overall survival rate. Currently, there is limited research specifically addressing the role of caspase-5 in OSCC. While caspase-5 is known to be involved in inflammatory responses and has been studied in other cancer types, its expression patterns and clinical significance in OSCC remain underexplored.

Collectively, these observations suggest that the NLRP3 inflammasome signaling may play a pivotal role in shaping the tumor microenvironment and influencing disease progression in OSCC, as supported in the available literature [60,61]. As with PD-1/PD-L1, previous studies

have suggested potential carcinogenic mechanisms associated with specific clinical variables such as poor oral hygiene. Interestingly, the association between poor oral hygiene and inflammasome marker expression may reflect the impact of chronic inflammation and dysbiosis in shaping a pro-tumorigenic microenvironment, consistent with prior studies linking microbial stimuli to inflammasome activation in OSCC [62]. More specifically, some studies have demonstrated that microorganisms associated with oral dysbiosis such as *P. gingivalis* can trigger NLRP3 activation and IL-1 β release in periodontal tissues [63], further supporting the pathogenic role that oral dysbiosis might have on OSCC carcinogenesis. Conversely, variables such as sex, smoking, alcohol use, or perineural invasion showed no significant correlation with these markers, underscoring the specificity of inflammasome-related pathways to clinical and environmental contexts.

In parallel, NAIP was also linked to the aforementioned clinical variables. However, to our best knowledge, there is limited evidence regarding the possible role of this protein and the NAIP/NLRC4 inflammasome in the context of OSCC. In HNSCC, NAIP expression is upregulated at both mRNA and protein levels compared to non-tumor tissues [64]. This overexpression has been significantly associated with poorer recurrence-free survival, suggesting that NAIP may play a role in tumor progression and immune evasion. While direct associations with clinical parameters such as tumor grade, vascular invasion, relapses, or poor oral hygiene have not yet been established, these findings imply that high NAIP expression could be linked to more aggressive tumor behavior and may influence the tumor immune microenvironment, as suggested in other types of epithelial tumors [65].

Overall, these findings support a growing body of evidence implicating inflammasomes—particularly NLRP3 and its associated effectors—as potential contributors to OSCC progression and possible targets for therapeutic modulation.

Insights from molecular markers correlations

The overall heatmap revealed a strong pattern of positive and significant correlations among the molecular markers across all patients, suggesting coordinated co-expression and the potential

activation of shared inflammatory or immunological pathways. When stratified by tumor grade, the heatmaps showed notable differences: tumors of grade 2 exhibited stronger and more numerous inter-marker correlations compared to grade 1. This shift indicates that as tumors become more aggressive, certain markers may become more functionally interconnected, potentially reflecting a network-level activation of molecular pathways involved in tumor progression.

In our stratified correlation analysis, we observed a marked increase in co-expression among molecular markers in tumor grade 2 compared to grade 1, with stronger and more widespread associations in higher-grade tumors. This pattern may reflect enhanced activation of shared inflammatory and immune-related pathways, such as the PD-1/PD-L1 axis involved in tumor immune evasion and the NLRP3 inflammasome complex, which mediates inflammatory responses through caspase activation and cytokine release (e.g., IL-1 β , IL-18). Notably, grade 2 tumors exhibited multiple perfect or near-perfect correlations, suggesting coordinated transcriptional regulation or network-level activation. However, these findings should be interpreted cautiously given the limited sample size and potential marker collinearity, highlighting the need for validation in larger, independent cohorts.

Strengths and weaknesses

One of the main strengths of our study lies in its integrative approach, combining detailed clinical data with robust immunohistochemical analysis of a broad panel of inflammasome-related markers and immune checkpoint proteins in OSCC tissue samples. By assessing both canonical and non-canonical NLRP3 inflammasome components—alongside PD-1/PD-L1 expression—we provide a comprehensive view of the tumor immune microenvironment and its correlation with key clinical variables. The observed perfect or near-perfect correlations in grade 2 tumors reflect co-expression patterns and limited within-group variability rather than statistical dependence among predictors in regression models. Furthermore, the inclusion of NAIP as a marker of the NAIP/NLRC4 inflammasome adds novelty to our work, expanding the current understanding of inflammasome activity in oral cancer. The systematic evaluation of multiple histopathological

and clinical parameters in relation to immune and inflammatory markers strengthens the interpretability and translational potential of our findings.

Despite these strengths, several limitations of this study should be acknowledged. First, the retrospective design and relatively small sample size ($n = 30$) may limit the generalizability of our findings and reduce statistical power, particularly for variables with low frequency. The limited sample size also affects the robustness of the statistical models employed. Specifically, binary logistic regression models must be interpreted with caution, as small datasets with sparse category distributions increase the risk of overfitting and may lead to numerical instability in parameter estimation. This is reflected in the large odds ratios and wide confidence intervals observed for some markers (e.g., Caspase-5, NAIP, NLRP3), which may partly arise from limited data support rather than truly large biological effect sizes. Consequently, regression-based associations should be regarded as exploratory rather than definitive.

Second, the observational nature of the study precludes causal inference, limiting our ability to establish directional biological relationships between clinical variables and molecular marker expression. Third, although immunohistochemistry provides valuable spatial and semi-quantitative information, it lacks the functional and mechanistic resolution offered by complementary approaches such as flow cytometry, multiplex imaging, or transcriptomic profiling, which could further elucidate inflammasome activation and immune checkpoint regulation. Likewise, potential confounding factors—including genetic variability, oral microbiome composition, environmental exposures, and prior treatment history—were not fully controlled and may influence inflammasome and PD-1/PD-L1 dynamics within the tumor microenvironment. Finally, another important limitation is that due to the nature of the study, we have not conducted a follow-up of the patients, and we have not been able to incorporate survival data, which would have substantially strengthened the clinical relevance of these findings.

To partially address concerns related to model instability, a sensitivity analysis was conducted in which all binary logistic regression models were re-estimated after verifying correct re-coding of

the two-level tumor grade variable. The markers identified as significant in the primary analysis (PD-L1, NAIP, NLRP3, Caspase-1, Caspase-5, and PYCARD) retained consistent effect directions and statistical significance, suggesting that these associations were not driven by variable misclassification or spurious collinearity. Because all binary logistic regression models were fitted as univariable models with a single molecular marker entered at a time, multicollinearity among predictors was not applicable, and variance inflation factors (VIF) were therefore not calculated. Nevertheless, given the sample size constraints, all regression findings should be interpreted with caution and require validation in larger, independent cohorts to establish reproducibility and clinical relevance.

Conclusions

In this study, we identified consistent associations between the histopathological expression of immune checkpoint proteins and inflammasome-related markers and key clinical features of OSCC, particularly tumor grade, relapse, vascular invasion, and oral hygiene status. The coordinated upregulation of PD-1/PD-L1 and components of both canonical and non-canonical NLRP3 inflammasome pathways—including NLRP3, PYCARD, caspases 1, 5, and 8, IL-1 β , IL-18, and NAIP—was predominantly observed in tumors with more aggressive clinical behavior, supporting the concept of a pro-inflammatory and immunomodulatory tumor microenvironment associated with disease progression. Conversely, better oral hygiene was consistently associated with lower expression of multiple immune and inflammatory markers, suggesting that local environmental and inflammatory conditions may modulate tumor-associated immune signaling alongside intrinsic tumor characteristics. The absence in this study of significant associations with other commonly evaluated clinical variables suggests the specificity of these pathways to particular pathological and microenvironmental contexts. Taken together, these findings provide integrative evidence linking immune checkpoint activity, inflammasome signaling, and clinically relevant features in OSCC, reinforcing the biological relevance of inflammatory and immune-re-

lated mechanisms in oral carcinogenesis while underscoring the need for further validation in larger and functionally oriented studies.

Acknowledgements

Author Contributions

All authors have read and agreed to the published version of the manuscript.

Conflict of interest statement

The authors declare no conflict of interest.

Funding sources

The study was supported by the Comunidad de Madrid (P2022/BMD-7321), ProACapital, and HALE KULANI, S. L. and MJR y FUNDACIÓN MUTUA MADRILEÑA.

References

1. Sun Z, Sun X, Chen Z, Du J, Wu Y. Head and Neck Squamous Cell Carcinoma: Risk Factors, Molecular Alterations, Immunology and Peptide Vaccines. *Int J Pept Res Ther*. 2021 Jan 1;28(1):19. <https://doi.org/10.1007/S10989-021-10334-5>. PubMed PMID: 34903958.
2. Badwelan M, Muaddi H, Ahmed A, Lee KT, Tran SD. Oral Squamous Cell Carcinoma and Concomitant Primary Tumors, What Do We Know? A Review of the Literature. *Current Oncology*. 2023 Apr 1;30(4):3721. <https://doi.org/10.3390/CURRONCOL30040283>. PubMed PMID: 37185396.
3. Bray F, Laversanne M, Sung H, Ferlay J, Siegel RL, Soerjomataram I, Jemal A. Global cancer statistics 2022: GLOBOCAN estimates of incidence and mortality worldwide for 36 cancers in 185 countries. *CA Cancer J Clin*. 2024 May 1;74(3):229–63. <https://doi.org/10.3322/CAAC.21834;REQUESTEDJOURNAL:JOURNALS:15424863;WGROU:STRING:PUBLICATION>. PubMed PMID: 38572751.
4. Sung H, Ferlay J, Siegel RL, Laversanne M, Soerjomataram I, Jemal A, Bray F. Global Cancer Statistics 2020: GLOBOCAN Estimates of Incidence and Mortality Worldwide for 36 Cancers in 185 Countries. *CA Cancer J Clin*. 2021 May 1;71(3):209–49. <https://doi.org/10.3322/CAAC.21660>. PubMed PMID: 33538338.
5. Yang J, Guo K, Zhang A, Zhu Y, Li W, Yu J, Wang P. Survival analysis of age-related oral squamous cell carcinoma: a population study based on SEER. *Eur J Med Res*. 2023 Dec 1;28(1):1–11. <https://doi.org/10.1186/S40001-023-01345-7/TABLES/3>. PubMed PMID: 37814268.
6. Nokovitch L, Maquet C, Crampon F, Taihi I, Roussel LM, Obongo R, Virard F, Fervers B, Deneuve S. Oral Cavity Squamous Cell Carcinoma Risk Factors: State of the Art. *J Clin Med*. 2023 May 1;12(9). <https://doi.org/10.3390/JCM12093264>.
7. Hashmi AA, Mudassir G, Rashid K, Malik UA, Zia S, Zia F, Irfan M. Risk Factors of Oral Squamous Cell Carcinoma with Special Emphasis on Areca Nut Usage and

- Its Association with Clinicopathological Parameters and Recurrence. *Int J Surg Oncol*. 2024;2024:9725822. <https://doi.org/10.1155/2024/9725822>. PubMed PMID: 39233744.
8. Rivera C, Venegas B. Histological and molecular aspects of oral squamous cell carcinoma (Review). *Oncol Lett*. 2014;8(1):7. <https://doi.org/10.3892/OL.2014.2103>. PubMed PMID: 24959211.
 9. Jyoti R, Vijay W, Preeti S, Lalita Y. Qualitative analysis of keratin in oral squamous cell carcinoma using alcian blue–periodic acid schiff, Ayoub-Shklar, and modified papanicolaou as special stains. *J Oral Maxillofac Pathol*. 2025 Jan 1;29(1):61. https://doi.org/10.4103/JOMFP.JOMFP_203_24. PubMed PMID: 40248631.
 10. Tan Y, Wang Z, Xu M, Li B, Huang Z, Qin S, Nice EC, Tang J, Huang C. Oral squamous cell carcinomas: state of the field and emerging directions. *Int J Oral Sci*. 2023 Dec 1;15(1):1–23. <https://doi.org/10.1038/S41368-023-00249-W>;SUBJMETA=1665,4028,631,67,692;KWRD=CANCER,ORAL+CANCER. PubMed PMID: 37736748.
 11. Sudhakara M, Reshma V, Khan N, Amulya SR. Uncommon features in conventional oral squamous cell carcinoma. *J Oral Maxillofac Pathol*. 2016 May 1;20(2):316. <https://doi.org/10.4103/0973-029-X.185905>. PubMed PMID: 27601830.
 12. Al-Rawi NH, Kawas S Al, Ani M Al, Alnuaimi AS, El-Sayed W, Alrashdan MS. Prediction of Lymphovascular and Perineural Invasion of Oral Squamous Cell Carcinoma by Combined Expression of p63 and Cyclin D1. *Eur J Dent*. 2023 Dec 29;17(4):1170. <https://doi.org/10.1055/S-0042-1760301>. PubMed PMID: 36716784.
 13. Colonia-García A, Salazar-Peláez LM, Serna-Ortiz CA, Álvarez-Sánchez LG, de Andrade CR. Prognostic value of lymphovascular and perineural invasion in squamous cell carcinoma of the tongue. *Oral Surg Oral Med Oral Pathol Oral Radiol*. 2022 Feb 1;133(2):207–15. <https://doi.org/10.1016/J.OOOO.2021.08.021>. PubMed PMID: 34758940.
 14. Hanahan D. Hallmarks of Cancer: New Dimensions. *Cancer Discov*. 2022 Jan 1;12(1):31–46. <https://doi.org/10.1158/2159-8290.CD-21-1059>. PubMed PMID: 35022204.
 15. Laliberté C, Ng N, Eymael D, Higgins K, Ali A, Kiss A, Bradley G, Magalhaes MAO. Characterization of Oral Squamous Cell Carcinoma Associated Inflammation: A Pilot Study. *Frontiers in Oral Health*. 2021 Sep 21;2:740469. <https://doi.org/10.3389/FROH.2021.740469/BIBTEX>
 16. Goertzen C, Mahdi H, Laliberte C, Meirson T, Eymael D, Gil-Henn H, Magalhaes M. Oral inflammation promotes oral squamous cell carcinoma invasion. *Oncotarget*. 2018 Jun 26;9(49):29047. <https://doi.org/10.18632/ONCOTARGET.25540>. PubMed PMID: 30018735.
 17. Tampa M, Mitran MI, Mitran CI, Sarbu MI, Matei C, Nicolae I, Caruntu A, Tocut SM, Popa MI, Caruntu C, Georgescu SR. Mediators of Inflammation – A Potential Source of Biomarkers in Oral Squamous Cell Carcinoma. *J Immunol Res*. 2018 Jan 1;2018(1):1061780. <https://doi.org/10.1155/2018/1061780>. PubMed PMID: 30539028.
 18. Pekarek L, Garrido-Gil MJ, Sanchez-Cendra A, Cassinello J, Pekarek T, Fraile-Martinez O, Garcia-Montero C, Lopez-Gonzalez L, Rios-Parra A, Alvarez-Mon M, Acero J, Diaz-Pedrero R, Ortega MA. Emerging histological and serological biomarkers in oral squamous cell carcinoma: Applications in diagnosis, prognosis evaluation and personalized therapeutics (Review). *Oncol Rep*. 2023 Dec 1;50(6):213. <https://doi.org/10.3892/OR.2023.8650>. PubMed PMID: 37859591.
 19. Ravindran S, Ranganathan S, R K, J N, A S, Kannan SK, Prasad K D, Marri J, K R. The role of molecular biomarkers in the diagnosis, prognosis, and treatment stratification of oral squamous cell carcinoma: A comprehensive review. *The Journal of Liquid Biopsy*. 2025 Mar 1;7:100285. <https://doi.org/10.1016/J.JLB.2025.100285>
 20. Ortega MA, Boaru DL, De Leon-Oliva D, Fraile-Martinez O, García-Montero C, Rios L, Garrido-Gil MJ, Barrena-Blázquez S, Minaya-Bravo AM, Rios-Parra A, Álvarez-Mon M, Jiménez-Álvarez L, López-González L, Guijarro LG, Diaz R, Saez MA. PD-1/PD-L1 axis: implications in immune regulation, cancer progression, and translational applications. *J Mol Med*. 2024 Aug 1;102(8):987–1000. <https://doi.org/10.1007/S00109-024-02463-3>. PubMed PMID: 38935130.
 21. Nocini R, Vianini M, Girolami I, Calabrese L, Scarpa A, Martini M, Morbini P, Marletta S, Brunelli M, Molteni G, Parwani A, Pantanowitz L, Eccher A. PD L1 in oral squamous cell carcinoma: A key biomarker from the laboratory to the bedside. *Clin Exp Dent Res*. 2022 Jun 1;8(3):690. <https://doi.org/10.1002/CRE2.590>. PubMed PMID: 35593124.
 22. Ortega MA, De Leon-Oliva D, García-Montero C, Fraile-Martinez O, Boaru DL, de Castro AV, Saez MA, Lopez-Gonzalez L, Bujan J, Alvarez-Mon MA, García-Honduvilla N, Diaz-Pedrero R, Alvarez-Mon M. Reframing the link between metabolism and NLRP3 inflammasome: therapeutic opportunities. *Front Immunol*. 2023;14:1232629. <https://doi.org/10.3389/FIMMU.2023.1232629>. PubMed PMID: 37545507.
 23. Bolívar BE, Brown-Suedel AN, Rohrman BA, Charendoff CI, Yazdani V, Belcher JD, Vercellotti GM, Flanagan JM, Bouchier-Hayes L. Noncanonical Roles of Caspase-4 and Caspase-5 in Heme-Driven IL-1 β Release and Cell Death. *J Immunol*. 2021 Apr 15;206(8):1878–89. <https://doi.org/10.4049/JIMMUNOL.2000226>. PubMed PMID: 33741688.
 24. Gurung P, Kanneganti TD. Novel Roles for Caspase-8 in IL-1 β and Inflammasome Regulation. *Am J Pathol*. 2015 Jan 1;185(1):17–25. <https://doi.org/10.1016/J.AJPATH.2014.08.025>. PubMed PMID: 25451151.
 25. Shadab A, Mahjoor M, Abbasi-Kolli M, Afkhami H, Moeinian P, Safdarian AR. Divergent functions of NLRP3 inflammasomes in cancer: a review. *Cell Communication and Signaling* 2023 21:1. 2023 Sep 15;21(1):1–15. <https://doi.org/10.1186/S12964-023-01235-9>. PubMed PMID: 37715239.
 26. Sharma BR, Kanneganti TD. NLRP3 inflammasome in cancer and metabolic diseases. *Nature Immunol*

- ogy 2021 22:5. 2021 Mar 11;22(5):550–9. <https://doi.org/10.1038/s41590-021-00886-5>. PubMed PMID: 33707781.
27. Kay C, Wang R, Kirkby M, Man SM. Molecular mechanisms activating the NAIP-NLRC4 inflammasome: Implications in infectious disease, autoinflammation, and cancer. *Immunol Rev.* 2020 Sep 1;297(1):67–82. <https://doi.org/10.1111/IMR.12906>. PubMed PMID: 32729154.
 28. Ortega MA, Pekarek L, Garcia-Montero C, Fraile-Martinez O, Saez MA, Asúnolo A, Alvarez-Mon MA, Monserrat J, Coca S, Toledo-Lobo MV, García-Honduvilla N, Albillos A, Buján J, Alvarez-Mon M, Guisjarro LG. Prognostic role of IRS-4 in the survival of patients with pancreatic cancer. *Histol Histopathol.* 2022 Feb 9;18432. <https://doi.org/10.14670/HH-18-432>. PubMed PMID: 35137378.
 29. García-Montero C, Fraile-Martinez O, Cobo-Prieto D, De Leon-Oliva D, Boaru DL, De Castro-Martinez P, Pekarek L, Gragera R, Hernández-Fernández M, Guisjarro LG, Toledo-Lobo MDV, López-González L, Díaz-Pedrero R, Monserrat J, Álvarez-Mon M, Saez MA, Ortega MA. Abnormal Histopathological Expression of Klotho, Ferroptosis, and Circadian Clock Regulators in Pancreatic Ductal Adenocarcinoma: Prognostic Implications and Correlation Analyses. *Biomolecules.* 2024 Aug 1;14(8):947. <https://doi.org/10.3390/BIOM14080947/S1>. PubMed PMID: 39199335.
 30. Ortega MA, Jiménez-álvarez L, Fraile-Martinez O, Garcia-Montero C, León-Oliva D De, Toledo-Lobo MDV, Palacios E, Granado P, Esteban A, Guisjarro LG, Pekarek L, Asúnolo Á, López-González L, Buján J, García-Honduvilla N, Álvarez-Mon M, Saez MA, Díaz-Pedrero R. Elevated tissue expression of RANKL and RANK is associated with poorer survival rates in pancreatic cancer patients. *Histol Histopathol.* 2024 Sep 1;39(9):1133–40. <https://doi.org/10.14670/HH-18-700>. PubMed PMID: 38230588.
 31. Munari E, Mariotti FR, Quatrini L, Bertoglio P, Tumino N, Vacca P, Eccher A, Ciompi F, Brunelli M, Martignoni G, Bogina G, Moretta L. PD-1/pd-l1 in cancer: Pathophysiological, diagnostic and therapeutic aspects. *Int J Mol Sci.* 2021 May 2;22(10). <https://doi.org/10.3390/IJMS22105123>. PubMed PMID: 34066087.
 32. Lin X, Kang K, Chen P, Zeng Z, Li G, Xiong W, Yi M, Xiang B. Regulatory mechanisms of PD-1/PD-L1 in cancers. *Mol Cancer.* 2024 Dec 1;23(1). <https://doi.org/10.1186/S12943-024-02023-W>. PubMed PMID: 38762484.
 33. Leporace-Jiménez F, Portillo-Hernandez I, Jiménez-Almonacid J, Rodríguez IZ, Mejía-Nieto M, Pedrero PC, Aniceto GS. Revisiting the Role of PD-L1 Overexpression in Prognosis and Clinicopathological Features in Patients with Oral Squamous Cell Carcinoma. *Onco* 2024, Vol 4, Pages 131-142. 2024 Jul 12;4(3):131–42. <https://doi.org/10.3390/ONCO4030011>
 34. Dave K, Ali A, Magalhaes M. Increased expression of PD-1 and PD-L1 in oral lesions progressing to oral squamous cell carcinoma: a pilot study. *Scientific Reports* 2020 10:1. 2020 Jun 16;10(1):1–11. <https://doi.org/10.1038/s41598-020-66257-6>. PubMed PMID: 32546692.
 35. Hirai M, Kitahara H, Kobayashi Y, Kato K, Bou-Gharios G, Nakamura H, Kawashiri S. Regulation of PD-L1 expression in a high-grade invasive human oral squamous cell carcinoma microenvironment. *Int J Oncol.* 2017 Jan 1;50(1):41–8. <https://doi.org/10.3892/IJO.2016.3785>. PubMed PMID: 27922697.
 36. Weber M, Wehrhan F, Baran C, Agaimy A, Büttner-Herold M, Preidl R, Neukam FW, Ries J. PD-L1 expression in tumor tissue and peripheral blood of patients with oral squamous cell carcinoma. *Oncotarget.* 2017;8(68):112584. <https://doi.org/10.18632/ONCO-TARGET.22576>. PubMed PMID: 29348848.
 37. Takahashi H, Sakakura K, Arisaka Y, Tokue A, Kaira K, Tada H, Higuchi T, Okamoto A, Tsushima Y, Chikamatsu K. Clinical and Biological Significance of PD-L1 Expression Within the Tumor Microenvironment of Oral Squamous Cell Carcinoma. *Anticancer Res.* 2019 Jun 1;39(6):3039–46. <https://doi.org/10.21873/ANTICANRES.13437>. PubMed PMID: 31177146.
 38. Lin YM, Sung WW, Hsieh MJ, Tsai SC, Lai HW, Yang SM, Shen KH, Chen MK, Lee H, Yeh KT, Chen CJ. High PD-L1 Expression Correlates with Metastasis and Poor Prognosis in Oral Squamous Cell Carcinoma. *PLoS One.* 2015 Nov 1;10(11):e0142656. <https://doi.org/10.1371/JOURNAL.PONE.0142656>. PubMed PMID: 26562534.
 39. Hsiao JR, Chang CC, Lee WT, Huang CC, Ou CY, Tsai ST, Chen KC, Huang JS, Wong TY, Lai YH, Wu YH, Hsueh WT, Wu SY, Yen CJ, Chang JY, Lin CL, Weng YL, Yang HC, Chen YS, Chang JS. The interplay between oral microbiome, lifestyle factors and genetic polymorphisms in the risk of oral squamous cell carcinoma. *Carcinogenesis.* 2018 May 28;39(6):778–87. <https://doi.org/10.1093/CARCIN/BGY053>. PubMed PMID: 29668903.
 40. Sukmana BI, Saleh RO, Najim MA, AL-Ghamdi HS, Achmad H, Al-Hamdani MM, Taher AAY, Alsalamy A, Khaleedi M, Javadi K. Oral microbiota and oral squamous cell carcinoma: a review of their relation and carcinogenic mechanisms. *Front Oncol.* 2024;14:1319777. <https://doi.org/10.3389/FONC.2024.1319777>. PubMed PMID: 38375155.
 41. Matsui K, Tani R, Yamasaki S, Ito N, Hamada A, Shintani T, Otomo T, Tokumaru K, Yanamoto S, Okamoto T. Analysis of Oral and Gut Microbiome Composition and Its Impact in Patients with Oral Squamous Cell Carcinoma. *Int J Mol Sci.* 2024 Jun 1;25(11):6077. <https://doi.org/10.3390/IJMS25116077/S1>. PubMed PMID: 38892262.
 42. Groeger S, Denter F, Lochnit G, Schmitz ML, Meyle J. Porphyromonas gingivalis Cell Wall Components Induce Programmed Death Ligand 1 (PD-L1) Expression on Human Oral Carcinoma Cells by a Receptor-Interacting Protein Kinase 2 (RIP2)-Dependent Mechanism. *Infect Immun.* 2020 Apr 1;88(5). <https://doi.org/10.1128/IAI.00051-20>. PubMed PMID: 32041789.
 43. Cui YX, Su XS. Clinicopathological Features of Programmed Cell Death-ligand 1 Expression in Patients with Oral Squamous Cell Carcinoma. *Open Medicine.*

- 2020 Apr 17;15(1):292. <https://doi.org/10.1515/MED-2020-0041>. PubMed PMID: 32337367.
44. Ratnakar S, Kumar M, Maurya MK, Qayoom S, Sagar M, Babu S, Kumar V. Expression of immune checkpoint protein in oral squamous cell carcinoma and its clinicopathological correlation: A tertiary care center cross-sectional study. *Journal of Oral and Maxillofacial Pathology*. 2023 Jul;27(3):597–597. https://doi.org/10.4103/JOMFP.JOMFP_169_22
 45. Mulder FJ, de Ruiter EJ, Gielgens T, Farshadpour F, de Bree R, van den Hout M, Kremer B, Willems SM, Speel E. Frequent PD-L1 expression in oral squamous cell carcinoma of non-smokers and non-drinkers, and association of tumor infiltrating lymphocytes with favorable prognosis. *Transl Oncol*. 2025 Mar 15;55:102357. <https://doi.org/10.1016/J.TRANON.2025.102357>. PubMed PMID: 40090069.
 46. Greeshma LR, Joseph AP, Sivakumar TT, Raghavan Pillai V, Vijayakumar G. Correlation of PD-1 and PD-L1 expression in oral leukoplakia and oral squamous cell carcinoma: an immunohistochemical study. *Scientific Reports* 2023 13:1. 2023 Dec 7;13(1):1–10. <https://doi.org/10.1038/s41598-023-48572-w>. PubMed PMID: 38066025.
 47. Kelley N, Jeltama D, Duan Y, He Y. The NLRP3 Inflammasome: An Overview of Mechanisms of Activation and Regulation. *Int J Mol Sci*. 2019 Jul 1;20(13). <https://doi.org/10.3390/IJMS20133328>. PubMed PMID: 31284572.
 48. Blevins HM, Xu Y, Biby S, Zhang S. The NLRP3 Inflammasome Pathway: A Review of Mechanisms and Inhibitors for the Treatment of Inflammatory Diseases. *Front Aging Neurosci*. 2022 Jun 10;14. <https://doi.org/10.3389/FNAGI.2022.879021>. PubMed PMID: 35754962.
 49. Tapia VS, Daniels MJD, Palazón-Riquelme P, Dewhurst M, Luheshi NM, Rivers-Auty J, Green J, Redondo-Castro E, Kaldis P, Lopez-Castejon G, Brough D. The three cytokines IL-1 β , IL-18, and IL-1 α share related but distinct secretory routes. *J Biol Chem*. 2019 May 5;294(21):8325. <https://doi.org/10.1074/JBC.RA119.008009>. PubMed PMID: 30940725.
 50. Garcia-Puente LM, Fraile-Martinez O, García-Montero C, Bujan J, De León-Luis JA, Bravo C, Rodríguez-Benitez P, Pintado P, Ruiz-Labarta FJ, Álvarez-Mon M, García-Honduvilla N, Cancelo MJ, Saez MA, Ortega MA. Placentas from Women with Late-Onset Preeclampsia Exhibit Increased Expression of the NLRP3 Inflammasome Machinery. *Biomolecules* 2023, Vol 13, Page 1644. 2023 Nov 13;13(11):1644. <https://doi.org/10.3390/BIOM13111644>. PubMed PMID: 38002326.
 51. Sánchez-Gil MA, Fraile-Martinez O, García-Montero C, De Leon-Oliva D, Boaru DL, De Castro-Martinez P, Camacho-Alcázar A, De León-Luis JA, Bravo C, Díaz-Pedrero R, López-Gonzalez L, Bujan J, Cancelo MJ, Álvarez-Mon M, García-Honduvilla N, Saez MA, Ortega MA. Exacerbated Activation of the NLRP3 Inflammasome in the Placentas from Women Who Developed Chronic Venous Disease during Pregnancy. *Int J Mol Sci*. 2024 May 1;25(10). <https://doi.org/10.3390/IJMS25105528>. PubMed PMID: 38791563.
 52. Bauer R, Rauch I. The NAIP/NLRC4 inflammasome in infection and pathology. *Mol Aspects Med*. 2020 Dec 1;76:100863. <https://doi.org/10.1016/J.MAM.2020.100863>. PubMed PMID: 32499055.
 53. Wang H, Luo Q, Feng X, Zhang R, Li J, Chen F. NLRP3 promotes tumor growth and metastasis in human oral squamous cell carcinoma. *BMC Cancer*. 2018 May 2;18(1):500. <https://doi.org/10.1186/S12885-018-4403-9>. PubMed PMID: 29716544.
 54. Jain T, Chandra A, Mishra SP, Khairnar M, Rajoria S, Maheswari R, Keerthika R, Tiwari S, Agrawal R. Unravelling the Significance of NLRP3 and IL- β 1 in Oral Squamous Cell Carcinoma and Potentially Malignant Oral Disorders: A Diagnostic and Prognostic Exploration. *Head Neck Pathol*. 2024 Dec 1;18(1). <https://doi.org/10.1007/S12105-024-01685-8>. PubMed PMID: 39141262.
 55. Wu CS, Chang KP, OuYang CN, Kao HK, Hsueh C, Chen LC, Cheng HY, Liang Y, Liou W, Liang C, Chang YS. ASC contributes to metastasis of oral cavity squamous cell carcinoma. *Oncotarget*. 2016;7(31):50074. <https://doi.org/10.18632/ONCOTARGET.10317>. PubMed PMID: 27367024.
 56. Li Y, Xu Z, Li J, Ban S, Duan C, Liu W. Interleukin-18 expression in oral squamous cell carcinoma: its role in tumor cell migration and invasion, and growth of tumor cell xenografts. *FEBS Open Bio*. 2018 Dec 1;8(12):1953. <https://doi.org/10.1002/2211-5463.12532>. PubMed PMID: 30524946.
 57. Liu PF, Hu YC, Kang BH, Tseng YK, Wu PC, Liang CC, Hou YY, Fu TY, Liou HH, Hsieh IC, Ger LP, Shu CW. Expression levels of cleaved caspase-3 and caspase-3 in tumorigenesis and prognosis of oral tongue squamous cell carcinoma. *PLoS One*. 2017 Jul 1;12(7). <https://doi.org/10.1371/JOURNAL.PONE.0180620>. PubMed PMID: 28700659.
 58. Li C, Egloff AM, Sen M, Grandis JR, Johnson DE. Caspase-8 mutations in head and neck cancer confer resistance to death receptor-mediated apoptosis and enhance migration, invasion, and tumor growth. *Mol Oncol*. 2014 Oct 1;8(7):1220–30. <https://doi.org/10.1016/J.MOLONC.2014.03.018>. PubMed PMID: 24816188.
 59. Uzunparmak B, Myers JN, Pickering CR. Loss of caspase-8 renders head and neck squamous cell carcinomas susceptible to necroptosis. *Clinical Cancer Research*. 2020 Jun 15;26(12_Supplement_2):B18–B18. <https://doi.org/10.1158/1557-3265.AACRAHNS19-B18>
 60. Agrawal S, Narang S, Shahi Y, Mukherjee S. Inhibitors of inflammasome (NLRP3) signaling pathway as promising therapeutic candidates for oral cancer. *Biochimica et Biophysica Acta (BBA) - General Subjects*. 2025 May 1;1869(6):130800. <https://doi.org/10.1016/J.BBAGEN.2025.130800>
 61. Shi R, Zhuang X, Liu T, Yao S nan, Xue F shan. The Role of NLRP3 Inflammasome in Oral Squamous Cell Carcinoma. *J Inflamm Res*. 2025 Apr 25;18:5601–9. <https://doi.org/10.2147/JIR.S512770>
 62. Yao Y, Shen X, Zhou M, Tang B. Periodontal Pathogens Promote Oral Squamous Cell Carcinoma by Regulating ATR and NLRP3 Inflammasome. *Front Oncol*. 2021 Sep 30;11:722797. <https://doi.org/10.3389/FONC.2021.722797/BIBTEX>

63. Ding PH, Yang MX, Wang NN, Jin LJ, Dong Y, Cai X, Chen LL. Porphyromonas gingivalis-Induced NLRP3 Inflammasome Activation and Its Downstream Interleukin-1 β Release Depend on Caspase-4. *Front Microbiol.* 2020 Aug 13;11:541276. <https://doi.org/10.3389/FMICB.2020.01881/BIBTEX>
64. Yu X, Cao W, Yang X, Yu C, Jiang W, Guo H, He X, Mei C, Ou C. Prognostic value and therapeutic potential of IAP family in head and neck squamous cell carcinoma. *Aging.* 2024 Feb 15;16(4):3674–93. <https://doi.org/10.18632/AGING.205551>. PubMed PMID: 38364254.
65. Domblides C, Crampton S, Liu H, Bartleson JM, Nguyen A, Champagne C, Landy EE, Spiker L, Profitt C, Bhattarai S, Grawe AP, Valenzuela MF, Lartigue L, Mahouche I, Dupaul-Chicoine J, Nishimura K, Lefort F, Decraecker M, Velasco V, Netzer S, Pitard V, Roy C, Soubeyran I, Racine V, Blanco P, Déchanet-Merville J, Saleh M, Canna SW, Furman D, Faustin B. Human NLRC4 expression promotes cancer survival and associates with type I interferon signaling and immune infiltration. *Journal of Clinical Investigation.* 2024 Jun 3;134(11). <https://doi.org/10.1172/JCI166085>. PubMed PMID: 38652550.

Supplementary figures

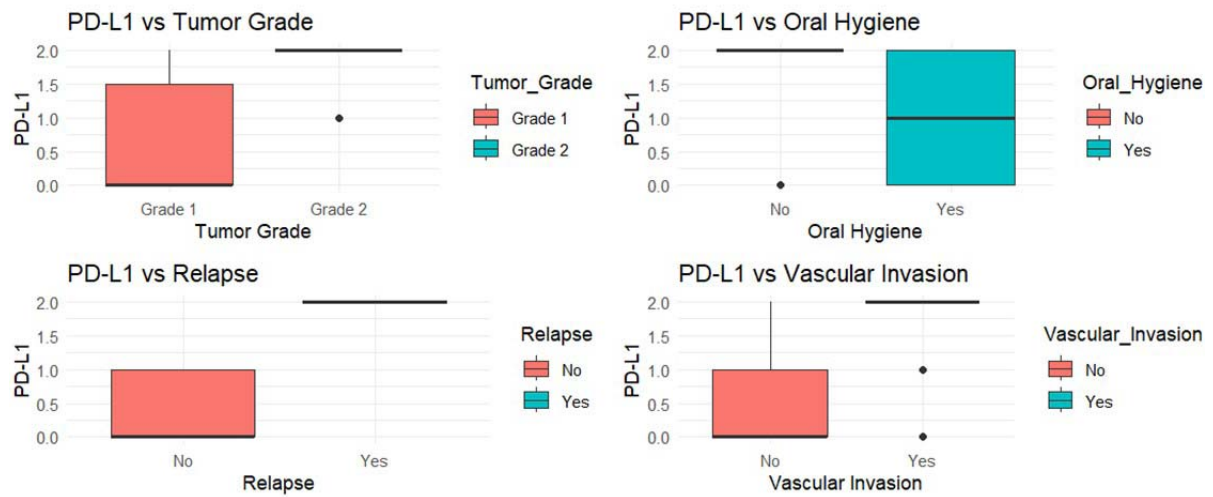


Figure S1.

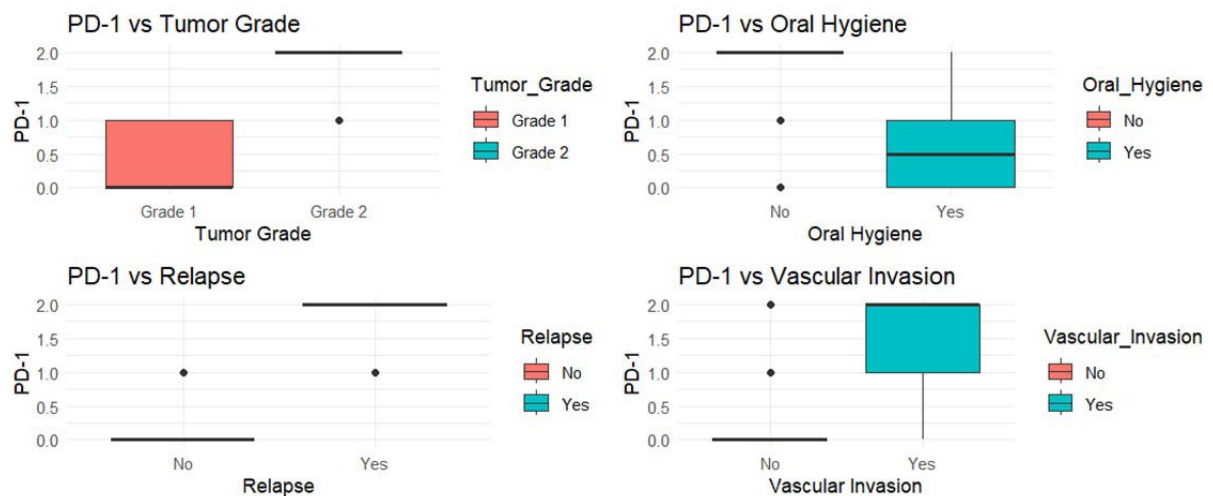


Figure S2.

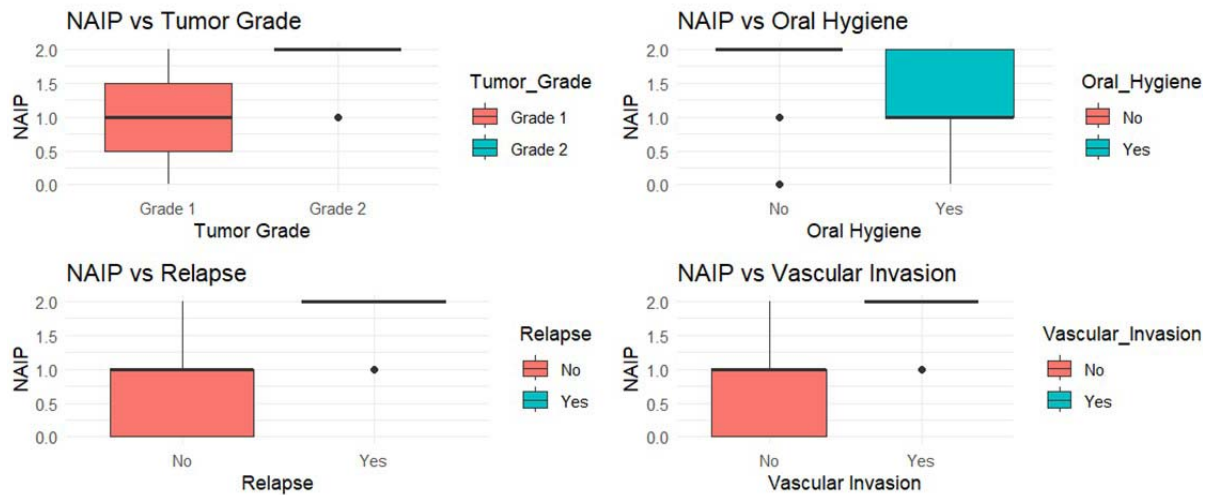


Figure S3.

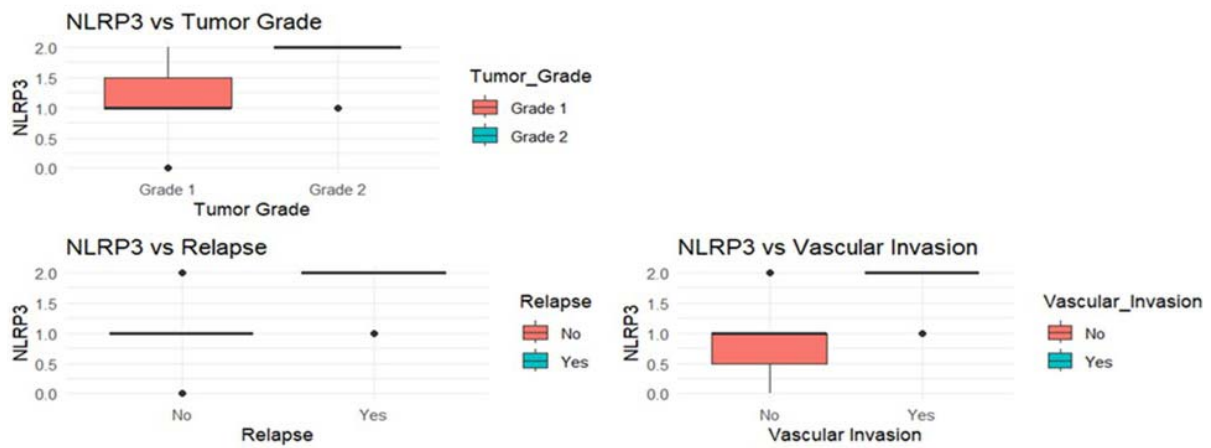


Figure S4.

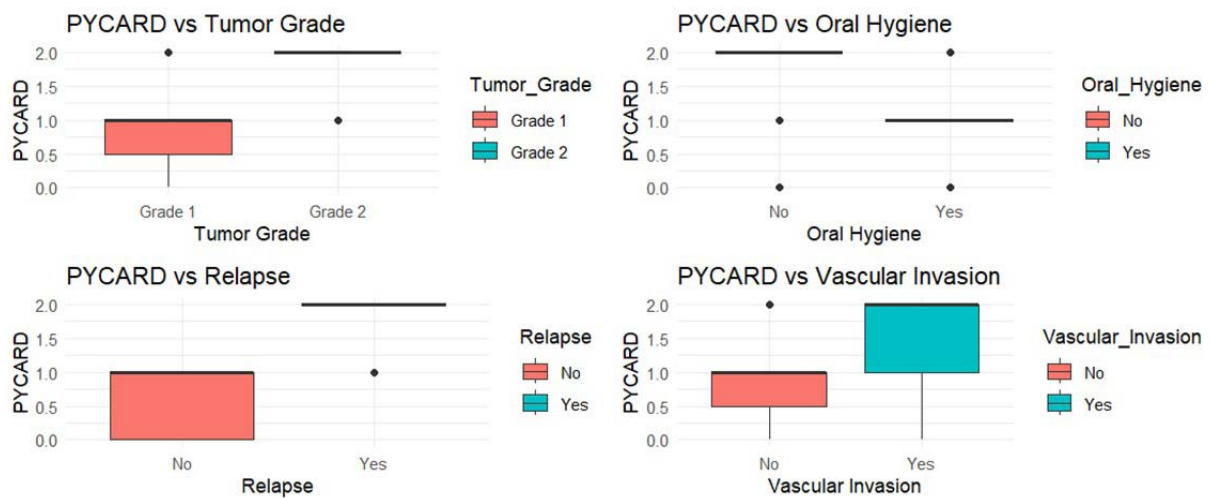


Figure S5.

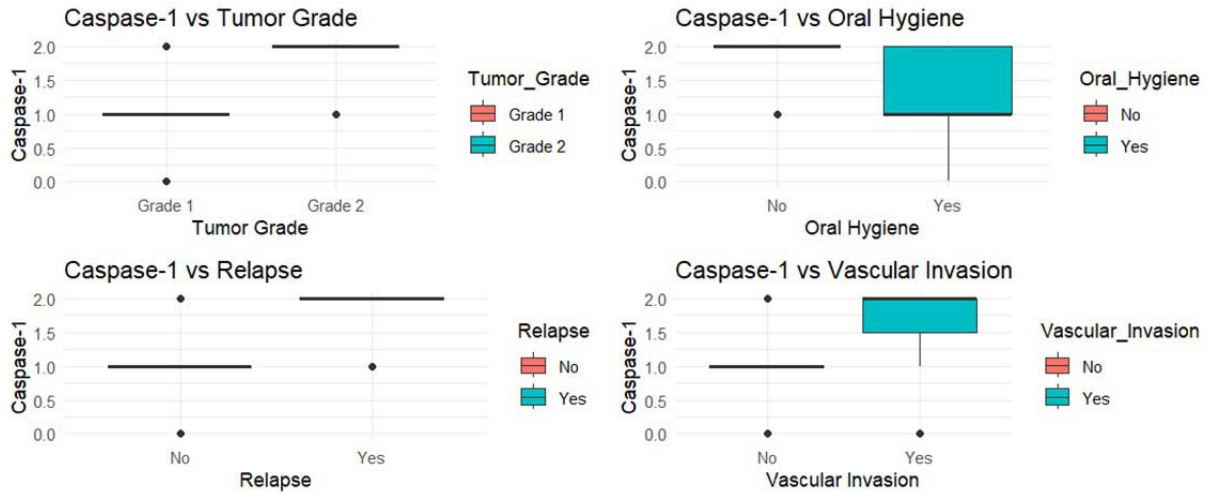


Figure S6.

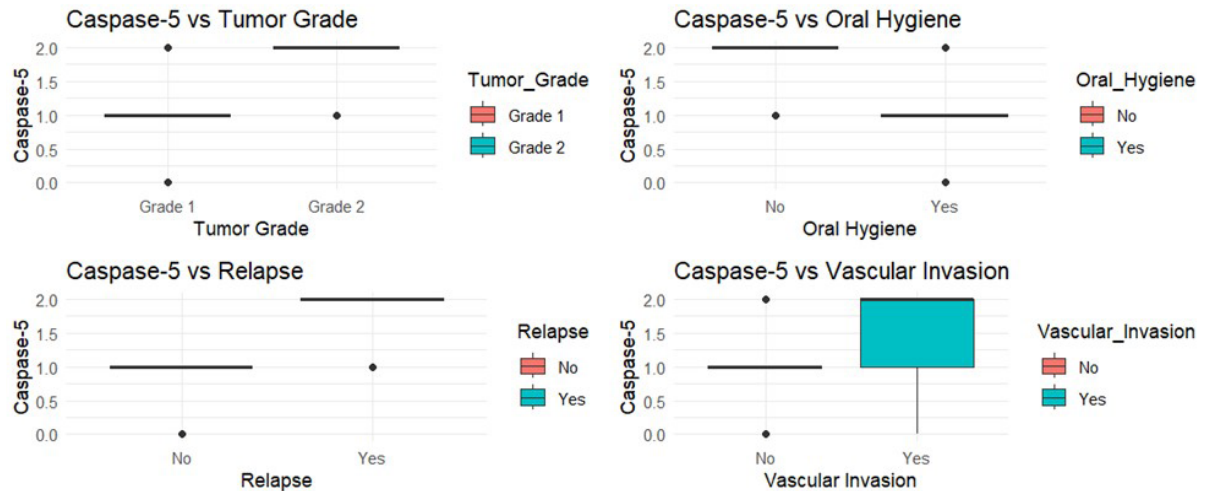


Figure S7.

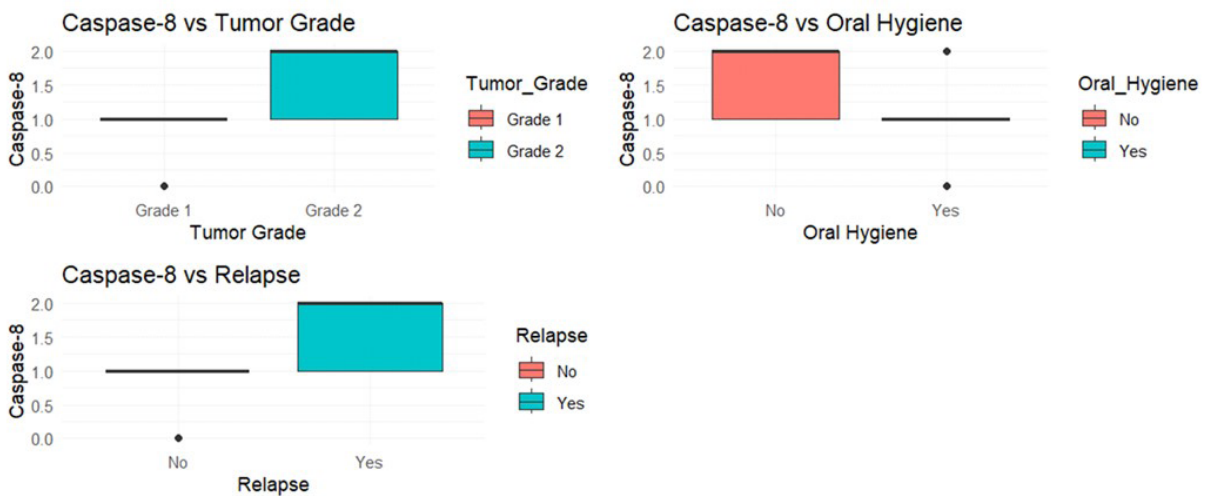


Figure S8.

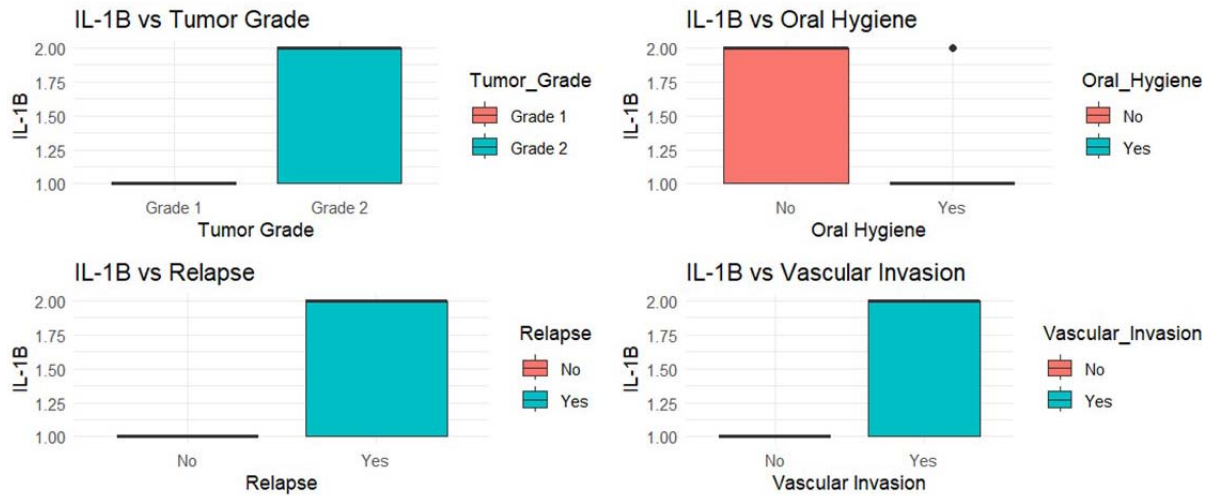


Figure S9.

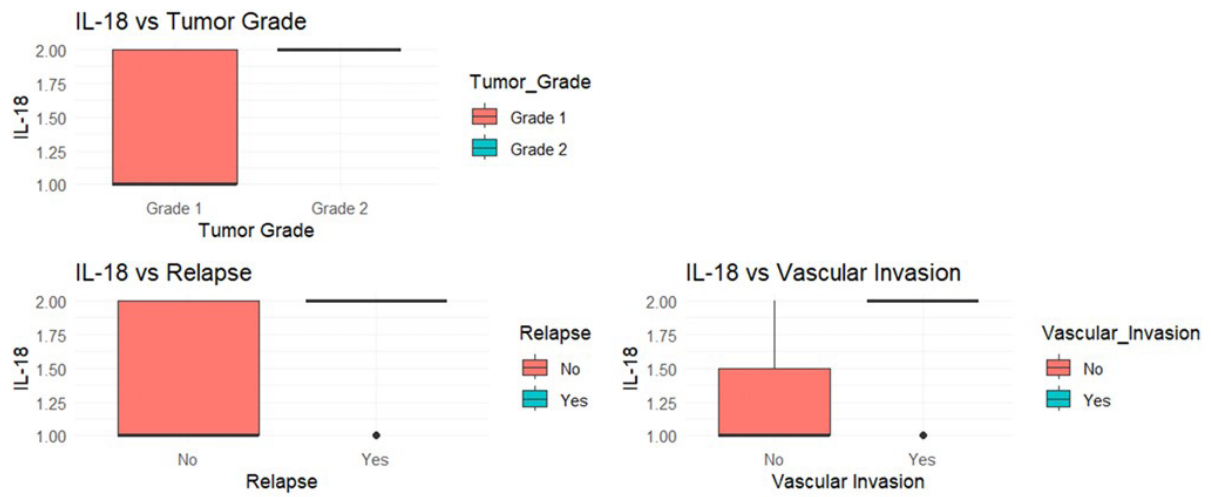


Figure S10.